Journal of Medicinal Chemistry

pubs.acs.org/jmc Article

Pyrazole Agonist of the Apelin Receptor Improves Symptoms of Metabolic Syndrome in Mice

Sanju Narayanan, Shaobin Wang, Vineetha Vasukuttan, Ravi Kumar Vyas Devambatla, Donghua Dai, Chunyang Jin, Rodney Snyder, Lucas Laudermilk, Scott P. Runyon,* and Rangan Maitra*

Cite This: *J. Med. Chem.* 2021, 64, 3006−3025 Read Online

ACCESS | Metrics & More | Article Recommendations | Supporting Information

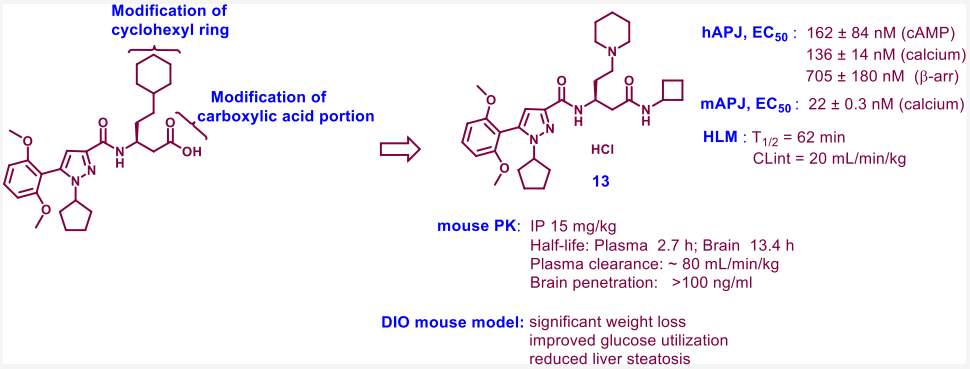

ABSTRACT: Apelin receptor agonism improves symptoms of metabolic syndrome. However, endogenous apelin peptides have short half-lives, making their utility as potential drugs limited. Previously, we had identified a novel pyrazole-based agonist scaffold. Systematic modification of this scaffold was performed to produce compounds with improved ADME properties. Compound **13** with favorable agonist potency (cAMPi EC_{50} = 162 nM), human liver microsome stability ($T_{1/2}$ = 62 min), and pharmacokinetic profile in rodents was identified. The compound was tested in a mouse model of diet-induced obesity (DIO) and metabolic syndrome for efficacy. Treatment with **13** led to significant weight loss, hypophagia, improved glucose utilization, reduced liver steatosis, and improvement of disease-associated biomarkers. In conclusion, a small-molecule agonist of the apelin receptor has been identified that is suitable for *in vivo* investigation of the apelinergic system in DIO and perhaps other diseases where this receptor has been implicated to play a role.

INTRODUCTION

Metabolic syndrome associated with obesity is a major problem in the developed world including the United States. Metabolic syndrome leads to type 2 diabetes, steatohepatitis, and cardiovascular diseases; these diseases together have a high mortality rate.[1] Therefore, new medications to treat metabolic syndrome are needed. The apelin receptor has emerged as a novel target for various important diseases including metabolic syndrome.[2] This class A GPCR is activated by two distinct classes of peptides—apelin and ELABELA. Activation of the receptor initiates downstream signaling primarily through the Gαi-dependent pathway, which inhibits cyclic adenosine monophosphate (cAMP) production and activates the extracellular signal-regulated kinase (ERK) signaling cascade. Termination of receptor signaling is through internalization of the apelin receptor via β-arrestin 1/2 recruitment.[3,4] These endogenous peptides of the apelin receptor are labile and not suitable for chronic dosing in patients suffering from metabolic syndrome and other diseases that require repeated administration of a therapeutic agent.[4] To date, small-molecule ligands of the apelin receptor have been under-reported in the literature.[5−11] Furthermore, the ones disclosed have little to no brain penetration. Both apelin and APJ are expressed in the central nervous system (CNS) and peripherally.[12,13] Strong expression of APJ is noted in the vasculature within endothelial cells but expression of APJ mRNA in other types of cells outside of the vasculature has also been reported.[13,14] Within the CNS, the receptor is expressed in the hypothalamus and other regions that are associated with hunger, satiety, motivation, and reward processing.[15,16] Therefore, central regulation of this receptor system could well be important beyond peripheral actions within the context of metabolic diseases.

Received: August 20, 2020
Published: March 11, 2021

https://dx.doi.org/10.1021/acs.jmedchem.0c01448
J. Med. Chem. 2021, 64, 3006−3025

Studies on the antiobesity and antidiabetic properties of the apelinergic system present a very intriguing picture.[17,18] Apelin is an adipokine that is produced and secreted by adipocytes.[19] Several reports indicate that circulating apelin levels are higher in obese and diabetic patients (reviewed in[17]) but not necessarily in patients with type 2 diabetes or gestational diabetes. These data indicate that hyperactivation of the apelinergic system is a possible consequence of obesity. Apelin is also an insulin sensitizer. Apelin lowered insulin secretion alone[20] or upon glucose stimulation[21] and improved glucose utilization in skeletal muscle cells of high-fat diet (HFD)-fed mice.[22,23] Apelin treatment also decreased body adiposity and serum levels of insulin and triglycerides in obese HFD-fed mice.[24] Apelin increased the serum adiponectin level and decreased leptin.[24] Furthermore, increased muscle fatty acid (FA) oxidation in response to apelin stimulation has been also described.[25] Loss of function studies support these observations. Apelin knockout (KO) mice on regular chow exhibit significantly higher insulin levels and glucose intolerance with increased abdominal fat and higher bodyweight than littermates (Figure 1). Administration

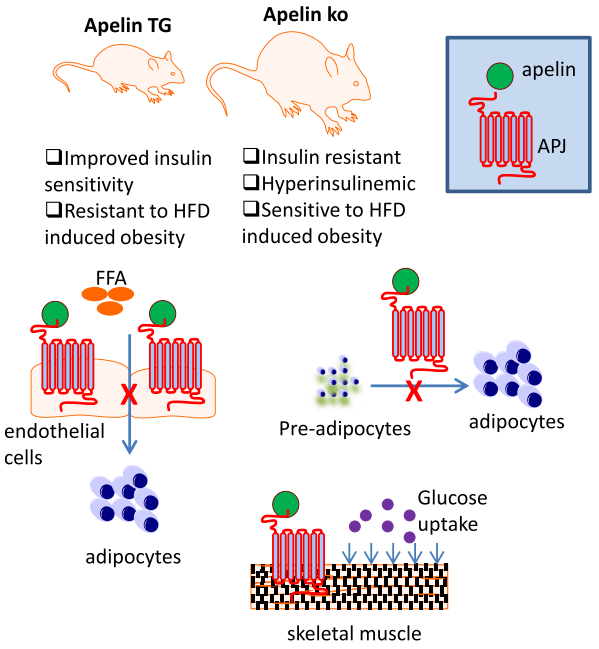

Figure 1. Role of an apelinergic system in DIO and metabolic syndrome. Apelin transgenic (TG) animals are insulin-sensitive and resistant to HFD-induced obesity compared to apelin knockout animals. APJ activation by apelin leads to the formation of large nonleaky vessels that combat hypertension and free FA transport. Apelin blocks differentiation of preadipocytes to adipocytes and improves glucose uptake in skeletal muscles. It also increases vascular mass.

of sucrose to KO animals exacerbates this phenotype, but these effects can be reversed by infusion of animals with Pyr-apelin-13.[26,27] Additional studies indicate that apelin, through its interaction with APJ receptor, can inhibit adipogenesis of preadipocytes and lipolysis in mature adipocytes (Figure 1).[28] Interestingly, both apelin and APJ are strongly expressed in endothelial cells. Endothelial cells play a key role in regulating FA transport and this process is affected by apelin and APJ. Activation of APJ by apelin leads to the formation of large, nonleaky lymphatic and blood vessels[29,30] that restrict the transport of FA and their uptake in adipose tissues (Figure 1).[31] In agreement with these data, apelin KO mice have vessels that are more amenable to FA transport.[31] Therefore, apelin KO animals on HFD with abnormal lymphatic and blood vessel enlargement are obese compared to littermates with normal apelin expression. Another report has indicated that apelin transgenic mice are resistant to diet-induced obesity (DIO) by virtue of increased vascular mass and mitochondrial biogenesis in skeletal muscles.[32]

In addition to these data, APJ activation by apelin has many beneficial effects on the cardiovascular system, which is a major problem in a large number of patients with metabolic syndrome. Every APJ KO line described to date suffers from heart failure due to pressure overload at an advanced age. They also demonstrate reduced angiogenic potential and develop vascular abnormalities.[29,30,33,34] Furthermore, reports indicate that apelin promotes recovery from ischemia, which is a hypoxic and vaso-occlusive disorder.[29] In reported clinical studies, acute Pyr-apelin-13 administration caused peripheral and coronary vasodilatation and increased cardiac output in human patients with chronic heart failure and also induced nitric oxide-dependent arterial vasodilation in healthy human volunteers without any adverse effects.[35−37] Interestingly, there are also reports suggesting that apelin has a positive ionotropic effect in the heart.[38,39] Taken together, APJ is a novel multimodal target for metabolic syndrome that is capable of diminishing insulin resistance, is antihypertensive, and has an inhibitory effect on DIO.[36,37]

Recently, we discovered and reported a potent pyrazole agonist **2** of the apelin receptor (cAMPi EC_{50} = 238 nM, Figure 2) through focused screening, which was further optimized to **3** (cAMPi EC_{50} = 97 nM).[11] However, compound **3** was not suitable for *in vivo* studies since it was rapidly metabolized (human liver microsome stability (HLM) $T_{1/2}$ = 6.25 min, CLint = 199 mL/min/kg), had poor solubility (<1 μM at pH 7.4), and was still too lipophilic. A small-molecule agonist that is suitable for *in vivo* investigation in DIO and possibly in animal models of other diseases modulated by the apelin receptor was needed.

RESULTS AND DISCUSSION

To improve pharmacokinetic (PK) properties of compound **3** (Figure 2) and to identify an *in vivo* metabolically stable compound, we started our SAR campaign first by replacing the lipophilic cyclohexyl moiety of compound **2**. Compounds with substituted alkyl/cycloalkyl amines replacing the cyclohexyl moiety in **2** were synthesized first (Table 1) to generate preliminary structure−activity relationships (SARs) and gain an understanding of receptor tolerances associated with these modifications and their effects on potency and efficacy. Alkyl and cycloalkyl amines provide a basic nitrogen that not only increases polarity but also improves solubility of compounds as hydrochloride salts. The agonist activity of synthesized analogues was evaluated using inhibition of forskolin-induced cAMP accumulation. In addition, recruitment of β-arrestin 2 was also evaluated as a measure of the desensitization potential of compounds.

At first, noncyclic diethyl amine-substituted **4** was synthesized and evaluated to monitor the influence of alkyl amine substitution on agonist potency (Table 1). The diethyl amine-substituted analogue **4** (cAMPi EC_{50} = 1365 nM) exhibited approximately sixfold reduced potency compared to the cyclohexyl analogue **2** (cAMPi EC_{50} = 238 nM). However, five-membered closed pyrrolidine ring analogue **5** was

https://dx.doi.org/10.1021/acs.jmedchem.0c01448
J. Med. Chem. 2021, 64, 3006−3025

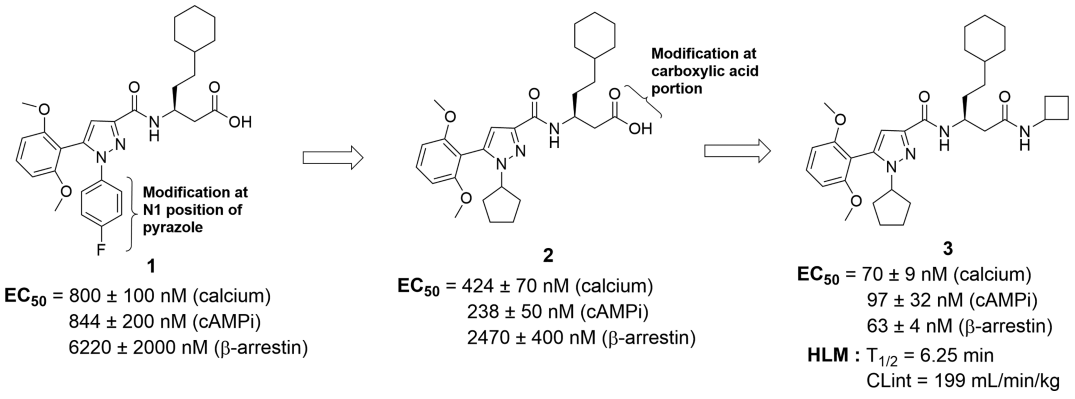

Figure 2. Chemical structure of initial lead **2** identified through focused screen and optimized to lead compound **3**.

Table 1. Modification of Cyclohexyl Moiety of 2

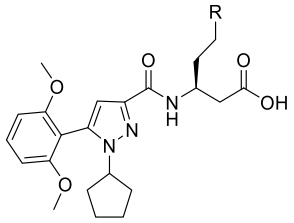

Compd.	R	Salt form	Apelin Receptor cAMPi, EC_{50}[a] nM±SEM (%E_{max})	Apelin Receptor β-arrestin2, EC_{50}[a] nM±SEM (%E_{max})
Pyr-Apelin-13	-	-	0.3 ± 0.10	1.0 ± 0.5
2	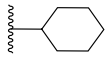	-	238 ± 50 (103)	2470 ± 400 (77)
4		HCl	1365 ± 352 (97)	>10,000
5		HCl	398 ± 127 (82)	>10,000
6		HCl	2110 ± 1400 (85)	5574± 1119 (68)
7	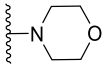	HCl	703 ± 185 (93)	>10,000
8	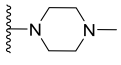	2HCl	805 ± 351 (61)	>10,000
9	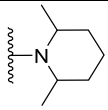	HCl	2112 ± 372 (91)	>10,000
10	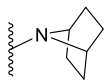	HCl	7562 ± 7536 (107)	>10,000
11	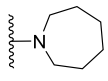	HCl	181 ± 71 (86)	3752 ± 1462 (82)

[*]EC_{50} values are averages of 2−3 experiments performed in duplicate unless otherwise stated ± standard error of the mean.

https://dx.doi.org/10.1021/acs.jmedchem.0c01448
J. Med. Chem. 2021, 64, 3006−3025

Table 2. Modification of the Cyclohexyl Moiety of 3

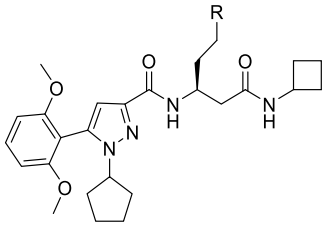

Compd.	R	Salt form	Apelin Receptor cAMPi, EC_{50} [a] nM±SEM (%E_{max})	Apelin Receptor β-arrestin2, EC_{50} [a] nM±SEM (%E_{max})	HLM	
					$T_{1/2}$ (min)	CL (mL/min/kg)
Pyr-Apelin-13	-	-	0.3 ± 0.10	1.0 ± 0.5	ND	ND
12		HCl	167± 44 (88)	2712 ± 341 (91)	NC	NC
13	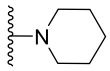	HCl	162 ± 84 (99)	705 ± 180 (88)	62	20
14	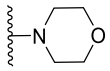	HCl	237 ± 51 (96)	1352 ± 245 (89)	17	73.1
15	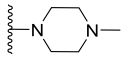	2HCl	721 ± 152 (83)	>10,000	ND	ND
16	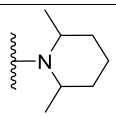	HCl	33 ± 1 (94)	459 ± 46 (87)	52	23.9
17	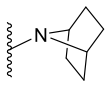	HCl	363 ± 148 (87)	4307 ± 385 (83)	ND	ND
18	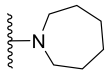	HCl	8 ± 3 (98)	159 ± 50 (87)	38	32.4

[*]EC_{50} values are averages of 2−3 experiments performed in duplicate unless otherwise stated ± standard error of the mean, NC—not calculated as no compound **12** peak detected in wells, ND—not done, HLM—human liver microsome stability, $T_{1/2}$—half-life, and CL—clearance.

equipotent (cAMPi EC_{50} = 398 nM) compared to **2** (cAMPi EC_{50} = 238 nM) indicating a preference for a cyclic ring structure for enhanced agonist potency. Increasing the hydrophobic volume to six carbon piperidine **6**, however, reduced the potency (cAMPi EC_{50} = 2110 nM) to ∼9-fold. This diminished potency was then rescued by the introduction of heteroatoms (O and N-Me) at the para position of the piperidine. Compounds **7** (cAMPi EC_{50} = 703 nM) and **8** (cAMPi EC_{50} = 805 nM) with morpholine and 4-methyl piperazine, respectively, exhibited ∼threefold improved potency compared to the piperidine analogue **6** (cAMPi EC_{50} = 2110 nM). Similarly, 2,6-dimethyl-substituted piperidine **9** was less potent (cAMPi EC_{50} = 2112 nM) indicating reduced receptor tolerance with compounds having six-membered heterocyclic ring systems. The cyclohexyl moiety in **2** was also replaced with a seven-membered bicyclic moiety, 7-azabicyclo[2.2.1]heptane **10**, to monitor the effect of steric bulk on agonist activity. However, the 7-azabicyclo[2.2.1]heptane substitution was not tolerated and reduced agonist potency (cAMPi EC_{50} = 7562 nM). Interestingly, the seven-membered azepane ring (**11**) exhibited enhanced agonist potency (cAMPi EC_{50} = 181 nM) compared to the cyclohexyl-substituted **2** indicating a preference for seven-membered hydrophobic cycloalkyl ring systems. Overall, five- or seven-membered cyclic heterocyclic rings (pyrrolidine and azepane) were well-tolerated and exhibited comparable or enhanced agonist potency relative to compound **2**. However, six-membered cycloalkyl derivatives (**6**, **7**, **8**, and **9**) exhibited reduced receptor tolerance and variable agonist potencies. *β*-Arrestin recruitment of these compounds was also investigated as a potential measure of desensitization.[40] Additionally, literature evidences also suggest a correlation between *β*-arrestin signaling and hypotensive effect *in vivo*.[41,42] Several compounds among **4**−**11** exhibited weak activity in the *β*-arrestin recruitment assay, with some showing no appreciable

https://dx.doi.org/10.1021/acs.jmedchem.0c01448
J. Med. Chem. 2021, 64, 3006−3025

recruitment at 10 μM, suggesting the possibility of low receptor internalization and desensitization with these analogues. This could improve the duration of action of these compounds and might be advantageous in a chronic disease setting requiring reduced or absent tolerance to an administered agent.

As noted earlier in Figure 2, conversion of cyclohexyl carboxylic acid **2** (cAMPi EC_{50} = 238 nM) to cyclobutyl amide **3** (cAMPi EC_{50} = 97 nM) enhanced the potency of the starting carboxylic acid scaffold. To monitor similar effects with the cycloalkyl amine-substituted cyclobutylamide scaffold, compounds **12**−**18** (Table 2) were synthesized. As previously observed (Figure 2), the five-membered cyclic pyrrolidine cyclobutylamide **12** (cAMPi EC_{50} = 167 nM) exhibited twofold enhanced potency relative to its carboxylic acid precursor **5** (cAMPi EC_{50} = 398 nM). Furthermore, increasing the hydrophobic volume to six-membered piperidine **13** (cAMPi EC_{50} = 162 nM) resulted in ∼13-fold enhanced potency compared to its carboxylic acid counterpart **6** (cAMPi EC_{50} = 2110 nM), indicating enhanced receptor interaction through cyclobutylamide substitution. However, compound **14** with a morpholine (cAMPi EC_{50} = 237 nM) did not show much improvement in potency relative to the carboxylic acid derivative **7** (cAMPi EC_{50} = 703 nM). Also, conversion of *N*-methyl piperazine carboxylic acid **8** (cAMPi EC_{50} = 805 nM) to cyclobutyl amide **15** (cAMPi EC_{50} = 721 nM) did not enhance potency suggesting that the presence of an additional H-bond acceptor did not enhance receptor interaction. Interestingly, 2,6-dimethyl-substituted piperidine **16** (cAMPi EC_{50} = 33 nM, ∼64-fold), 7-azabicyclo[2.2.1]heptane **17** (cAMPi EC_{50} = 363 nM, 21-fold), and seven-membered azepane cyclobutylamide **18** (cAMPi EC_{50} = 8 nM, ∼23-fold) substitutions significantly enhanced potency compared to their carboxylic acid precursors. β-Arrestin recruitment of these compounds was also investigated. Compounds with piperidine (**13**, βarr EC_{50} = 705 nM), 2,6-dimethyl piperidine (**16**, βarr EC_{50} = 459 nM), and azepane (**18**, βarr EC_{50} = 159 nM) also recruited β-arrestin with an EC_{50} value < 1 μM (Table 2). Since our goal was to develop potent and metabolically stable compounds suitable for *in vivo* study, the stability of select potent compounds **13**, **14**, **16**, and **18** was evaluated in the HLM stability assay (Table 2). Compound **13** exhibited the most favorable HLM stability ($T_{1/2}$ = 62 min) and clearance (CL_{INT} = 20 mL/min/kg) suggesting the importance of the piperidine moiety for improved metabolic stability. Therefore, this compound was selected for further evaluation versus the more potent compounds.

Since compound **13** with a piperidine moiety exhibited the most favorable HLM stability, we continued with this scaffold for our next round of optimization to identify compounds with improved potency and metabolic stability. Diverse polar and nonpolar substituted amides and nonamide derivatives were synthesized to monitor the effect in agonist potency and metabolic stability of these compounds (Table 3). Compound **19** with cyclobutyl ester (Table 3) was synthesized to explore the importance of the amide nitrogen in **13** for agonist potency. Substituting NH with O did not reduce the agonist potency suggesting that the amide nitrogen may not be critical for preserving the agonist activity. Considering the metabolic liability of the cyclobutylamide moiety, we synthesized compounds **20** (3, 3-difluorocyclobutylamide), **21** (*N*-methyl cyclobutylamide), **22** (1-methylcyclobutylamide), and **23** (1-methyloxetanamide) that blocked the possible metabolic sites with the incorporation of heteroatoms (F and O) and a methyl group. Compounds **20** (cAMPi EC_{50} = 9 nM) and **21** (cAMPi

Table 3. Modification of the Carboxylic Acid Moiety of 6

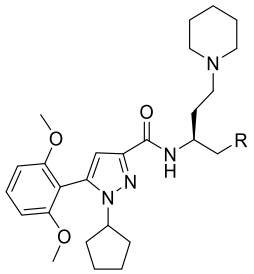

Compd.	R	Apelin Receptor cAMPi, EC_{50} [a] nM±SEM (%E_{max})	Apelin Receptor β-arrestin2, EC_{50} [a] nM±SEM (%E_{max})	HLM	
				$T_{1/2}$ (min)	CL (mL/min/kg)
Pyr-Apelin-13	-	0.3 ± 0.10	1.0 ± 0.5	ND	ND
6	-	2110 ± 1400 (85)	5574± 1119 (68)	ND	ND
13	-	162 ± 84 (99)	705 ± 180 (88)	62	20
19		285 ± 0.03 (97)	101 ± 7 (91)	ND	ND
20	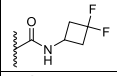	9 ± 2 (108)	158 ± 45 (103)	38	32.4
21	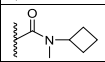	105 ± 7 (90)	326 ± 41 (84)	37	33.3
22	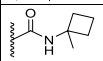	352 ± 150 (86)	1426 ± 96 (83)	ND	ND
23	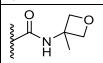	241 ± 91 (87)	3399 ± 172 (91)	ND	ND
24		5000 ± 809 (99)	>10,000	ND	ND
25	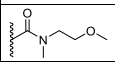	2411 ± 1057 (92)	>10,000	ND	ND
26	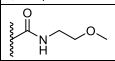	1185 ± 442 (90)	8921 ± 1367 (88)	ND	ND
27	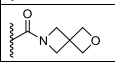	5892 ± 2642 (106)	>10,000	ND	ND
28	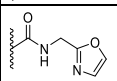	194 ± 106 (91)	827 ± 132 (95)	ND	ND
29	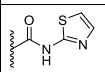	1 ± 0.14 (87)	12 ± 2 (93)	27	46.7
30	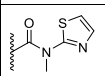	5 ± 1 (112)	14 ± 0.205 (117)	37	33.4
31	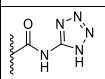	93 ± 43 (87)	391 ± 151 (89)	24.2	25.8
32	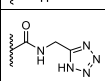	693 ± 322 (94)	1801 ± 462 (79)	ND	ND
33	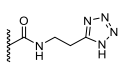	2642 ± 1455 (104)	7301 ± 991 (92)	ND	ND
34		134 ± 62 (94)	523 ± 0.4 (99)	33	37.8
35		779 ± 375 (92)	2316 ± 46 (93)	ND	ND

[a]EC_{50} values are averages of 2−3 experiments performed in duplicate unless otherwise stated ± standard error of the mean, ND—not done, HLM—human liver microsome stability, $T_{1/2}$—half-life; and CL—clearance.

https://dx.doi.org/10.1021/acs.jmedchem.0c01448
J. Med. Chem. 2021, 64, 3006−3025

Table 4. *In vitro* Screening and ADMET Profiling of 13

compd.	calcium (human) EC50[a] nM ± SEM (% E_{max})	calcium (mouse) EC50[a] nM ± SEM (% E_{max})	[^{35}S]GTPγS EC_{50}[a] nM ± SEM (% E_{max})	binding (human) Ki[a] nM ± SEM	hERG (10 μM)	AT1 calcium EC50 (μM)	solubility (μM, pH 7.4)	MDCK A−B ratio (%)	plasma protein binding (human) (%)[b]
13	136 ± 14 (91)	22 ± 0.3 (94)	483 ± 44 (116)	90 ± 3	inactive	>10	192	9.6	91

[a]EC_{50} and K_i values are averages of 2−3 experiments performed in duplicate unless otherwise stated ± standard error of the mean. [b]Propanolol was used as a positive control with ∼61% PPB.

Table 5. PK Analyses of 13[a]

species	route	dose (mg/kg)	C_{max} (ng/mL)		AUC_{all} (h·ng/mL)	CL (mL/min/kg)	T1/2 (h)
mouse	IP	15	plasma	1580	2998	83	2.7
			brain	103	1075	169	13.4

[a]C_{max}—maximum concentration, $T_{1/2}$—half-life, CL—clearance, and AUC—area under the curve.

Scheme 1. Synthesis of Compound 13[a]

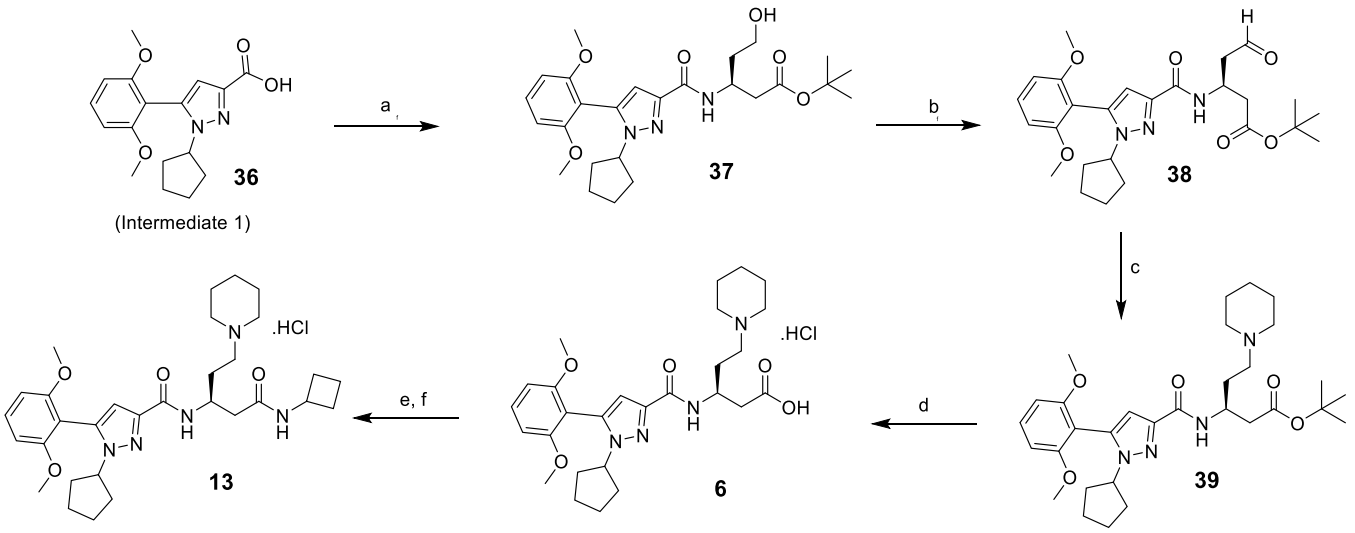

[a]Reagents and conditions: (a) (*S*)-*tert*-butyl 3-amino-5-hydroxypentanoate (**47**, Intermediate 2), HBTU, Et_3N, CH_3CN, 16 h, 45%; (b) Dess−Martin periodinane, DCM, 1 h, 98%; (c) piperidine, $NaBH(OAc)_3$, DCE, RT, 16 h, 61%; (d) 4 M HCl in dioxane, DCM, RT, 8 h; (e) cyclobutylamine, HBTU, CH_3CN, RT, 4 h, 87%; (f) 2 M HCl in ether, MeOH, 0 °C to RT, 30 min.

EC_{50} = 105 nM) exhibited enhanced agonist potency compared to **13** (cAMPi EC_{50} = 162 nM), however were surprisingly metabolized faster (**20**: HLM $T_{1/2}$ = 38 min; **21**: HLM $T_{1/2}$ = 37 min) than **13** (HLM $T_{1/2}$ = 62 min) suggesting emergence of additional liabilities due to these substitutions.

Further in our quest to identify more potent and stable analogues, we synthesized analogues substituting the cyclobutyl moiety with various alkyl, cycloalkyl, and heterocyclic groups. Compounds **26** (cAMPi EC_{50} = 1185 nM) and **25** (cAMPi EC_{50} = 2411 nM) with 2-methoxyethylamide and *N*-methyl, 2-methylethylamide substitutions (Table 3), respectively, did not enhance potency compared to **13** (cAMPi EC_{50} = 162 nM). Similarly, compound **27** with 2-oxa-6-azaspiro[3.3]heptane amide substitution (cAMPi EC_{50} = 5892 nM) also exhibited poor potency compared to **13** (cAMPi EC_{50} = 162 nM). Diverse heterocyclic amides (**28**, **29**, **30**, **31**, **32**, and **33**) (oxazole, thiazole, and tetrazole) were also synthesized and evaluated for agonist potency. Compounds **29** (cAMPi EC_{50} = 1 nM), **30** (cAMPi EC_{50} = 5 nM), and **31** (cAMPi EC_{50} = 93 nM) were more potent than **13** (cAMPi EC_{50} = 162 nM), however were metabolized (**29**: HLM $T_{1/2}$ = 27 min; **30**: HLM $T_{1/2}$ = 37 min; **31**: HLM $T_{1/2}$ = 24.2 min) rapidly compared to **13** (HLM $T_{1/2}$ = 62 min). In addition, analogues lacking the amide with direct heterocyclic substitutions (**34**, 1,2,4-triazole; **35**, 1,3,4-oxadiazole) were synthesized and evaluated for agonist potency (Table 3). Among these, compound **34** (cAMPi EC_{50} = 134 nM) exhibited improved potency, however it was metabolically less stable (HLM $T_{1/2}$ = 33 min) than **13** (HLM $T_{1/2}$ = 62 min). β-Arrestin recruitment of these compounds was also evaluated. Compounds with cyclobutyl ester (**19**, βarr EC_{50} = 101 nM), 3,3-difluorocyclobutylamide (**20**, βarr EC_{50} = 158 nM), *N*-methyl, *N*-cyclobutylamide (**21**, βarr EC_{50} = 326 nM), *N*-thiazolylamide (**29**, βarr EC_{50} = 12 nM), and *N*-methyl, *N*-thiazolylamide (**30**, βarr EC_{50} = 14 nM) activated the β-arrestin pathway with an EC_{50} value < 0.5 μM (Table 3). Overall, since compound **13** exhibited favorable agonist potency (cAMPi EC_{50} = 162 nM) and HLM stability (HLM $t_{1/2}$ = 62 min, CL_{INT} = 20 mL/min/kg), we proceeded with this compound for broad *in vitro* screening and ADMET profiling (Table 4).

Compound **13** exhibited a *K*i of 90 nM and high agonist potency (Ca^{2+} EC_{50} = 22 nM) at a mouse APJ receptor (calcium mobilization CHO-$G_{\alpha q16}$ cells stably expressing mouse APJ). In addition, compound **13** was not active in the hERG assay with <50% inhibition at 10 μM as determined by displacement of radiolabeled astemizole using membrane preparation from PerkinElmer.[43] Potential off-target activity of **13** was independ-

https://dx.doi.org/10.1021/acs.jmedchem.0c01448
J. Med. Chem. 2021, 64, 3006−3025

Scheme 2. Synthesis of 1-Cyclopentyl-5-(2,6-dimethoxyphenyl)-1*H*-pyrazole-3-carboxylic Acid (Intermediate 1)[11a]

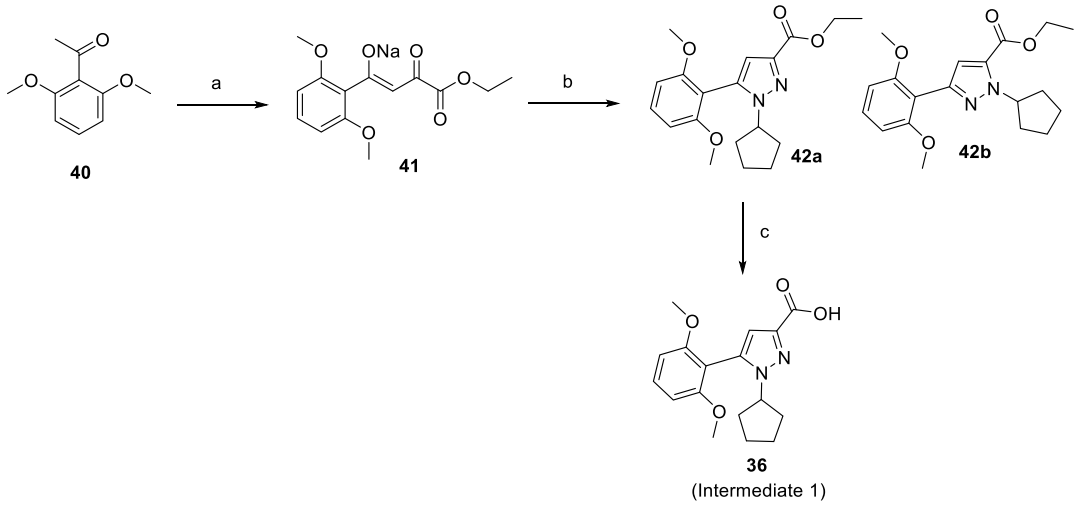

[a]Reagents and conditions: (a) Diethyl oxalate, NaOEt, EtOH, reflux, 4 h; 97% (b) cyclopentylhydrazine trifluoroacetate, glacial acetic acid, conc. HCl, reflux,3 h; 73% (c) LiOH·H_2O, MeOH/THF/H_2O, RT, 18 h, 98%.

Scheme 3. Synthesis of (*S*)-*tert*-Butyl 3-Amino-5-hydroxypentanoate (Intermediate 2)[46a]

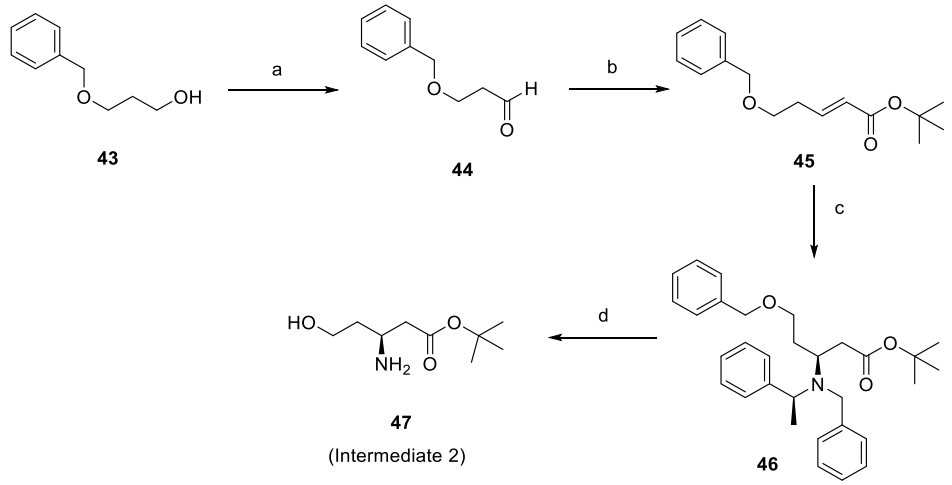

[a]Reagents and conditions: (a) Dess−Martin periodinane, DCM, 0 °C to RT, 3 h, 98% (b) $(EtO)_2POCH_2CO_2{}^tBu$, BuLi, THF, −78° C to RT, 1 h; 61% (c) (*S*)-*N*-benzyl-*N*-α-methyl-benzylamine, BuLi, THF, −78 °C, 3 h; 60% (d) 10% Pd/C, H_2, 50 psi, 20% acetic acid in EtOH, RT, 48 h, 88%.

ently determined by Eurofin PanLabs against several targets including receptors and ion channels. At 10 μM test concentration, compound **13** showed minimal cross reactivity to most receptors tested. Approximately >50% inhibition of binding was noted at few receptors and ion channels (see the Supporting Information). Furthermore, IC_{50} determination at these receptors revealed weak off-target activity at these receptors (see the Supporting Information). Plasma protein binding (human) was also undertaken for compound **13** and was ∼91% bound (Rapid Equilibrium Dialysis method with LC−MS detection, Thermo Fisher kit).[44] This compound demonstrated limited transport across monolayers of MDCK-mdr1 cells predicting low but positive brain penetration and was not active at the AT1 receptor.[45] Furthermore, this compound was negative in Ames assay suggesting low carcinogenic potential (data not shown).

Based on data generated *in vitro*, **13** was deemed suitable for *in vivo* exploration. PK evaluation was performed in mice that were administered a dose of 15 mg/kg of **13** via intraperitoneal injection (IP). Samples were collected in multiple time points (0.5, 1, 2, 4, 8, and 24 h) to obtain plasma and brain maximum concentrations. Compound **13** demonstrated (Table 5) reasonable half-life (2.7 h in plasma and 13.4 h in brain), clearance (∼80 mL/min/kg in plasma), and brain penetration (>100 ng/mL based on Cmax). Based on cumulative data, a BID dosing regimen was envisioned with this compound for *in vivo* studies in the DIO model of metabolic syndrome.

Chemistry. Compound **13** was synthesized in five steps, as shown in Scheme 1. Coupling of 1-cyclopentyl-5-(2,6-dimethoxyphenyl)-1*H*-pyrazole-3-carboxylic acid **36** (Intermediate 1, Scheme 2) with (*S*)-*tert*-butyl 3-amino-5-hydroxypentanoate (Intermediate 2, Scheme 3) using the HBTU coupling reagent provided the *O*-*tert* butyl-protected intermediate **37**. Primary alcohol in intermediate **37** was then subsequently oxidized to aldehyde **38** using the Dess−Martin periodinane oxidizing reagent. The aldehyde then underwent reductive amination with piperidine to provide intermediate **39** in good yields. Deprotection of *tert*-butyl ester in **39** using 4 M

https://dx.doi.org/10.1021/acs.jmedchem.0c01448
J. Med. Chem. 2021, 64, 3006−3025

Scheme 4. Synthesis of Compounds 4−11 and 12−18[a]

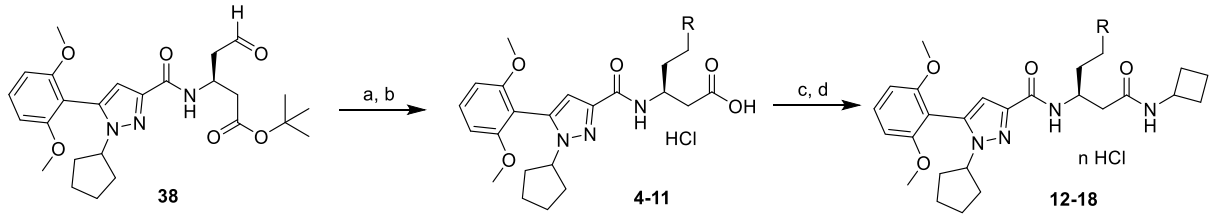

[a]Reagents and conditions: (a) cycloalkyl amine (R−NH), $NaBH(OAc)_3$, DCE, RT, 16 h; (b) 4 M HCl in dioxane, DCM, RT; (c) cyclobutylamine, HBTU, CH_3CN, RT, 3 h; (d) 2 M HCl in ether, MeOH, 0 °C to rt, 30 min.

Scheme 5. Synthesis of 34 and Amide Analogues 20−33[a]

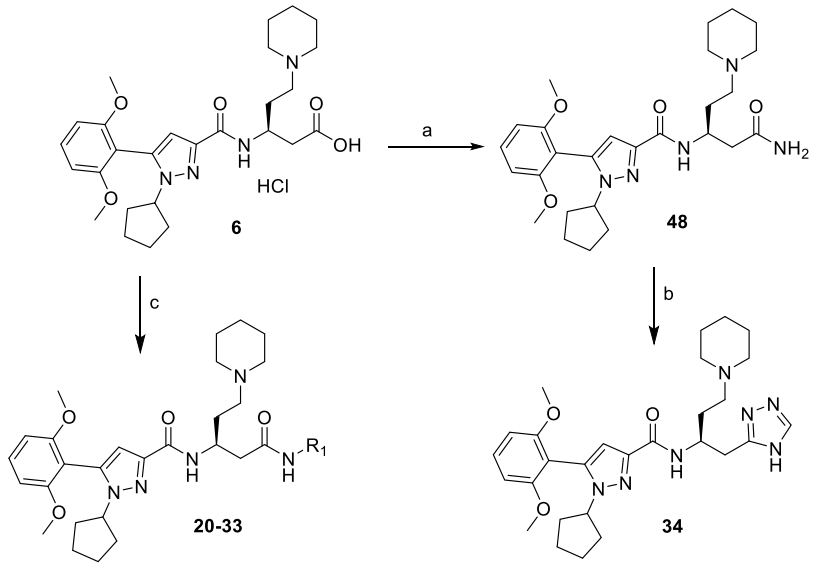

[a]Reagents and conditions: (a) ammonium carbonate, Boc_2O, pyridine, dioxane, 12 h, 69%; (b) DMF−DMA, 120 °C, 2 h; $NH_2NH_2{\cdot}H_2O$, CH_3COOH, 90 °C, 2 h, 57%; (c) R_1−NH_2, HBTU, MeCN, RT, 4 h.

Scheme 6. Synthesis of Analogue 35[a]

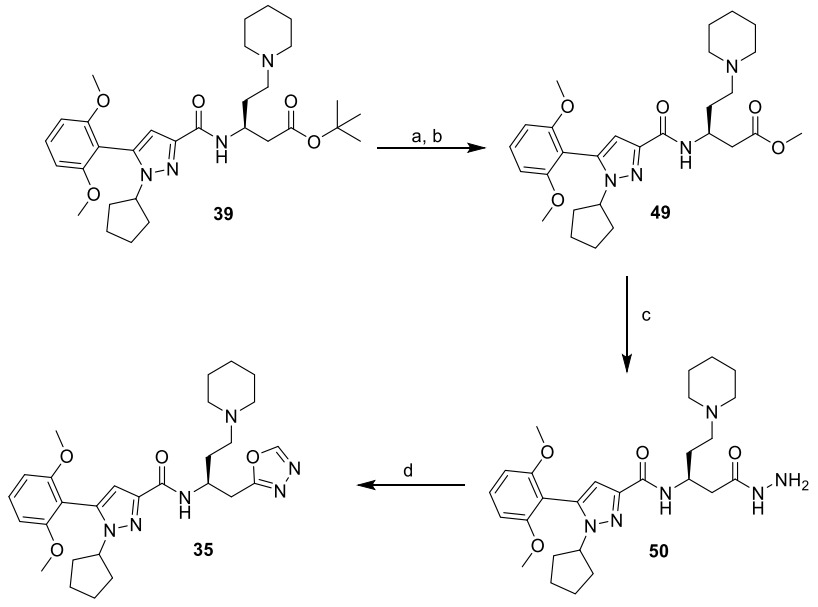

[a]Reagents and conditions: (a) TFA, DCM, RT, 2 h, crude; (b) MeOH, H_2SO_4, RT, 15 h, crude; (c) $NH_2NH_2{\cdot}H_2O$, EtOH, 80 °C, 3 h, 55%; (d) $CH(OMe)_3$, PTSA·H_2O, 85 °C, 2 h, 59%.

https://dx.doi.org/10.1021/acs.jmedchem.0c01448
J. Med. Chem. 2021, 64, 3006−3025

Table 6. Compound 13 Improves Biomarkers Associated with Metabolic Syndrome in DIO Mice[a]

biomarker	treatment groups			
	ND + vehicle	HFD + vehicle	HFD + comp **13** (5 mg/kg)	HFD + comp **13** (15 mg/kg)
bodyweight (% of baseline)	94.0 (1.0)	98.5 (1.2)	94.2 (1.3)*	82.0 (1.8)**
daily food consumption (g)	2.6 (0.2)	2.5 (0.3)	2.5 (0.3)	1.8 (0.2)*
fat pad weight (total, g)	0.87 (0.2)**	1.98 (0.12)	1.38 (0.38)	0.43 (0.07)*
fructosamine (μmol)	1028.4 (46.2)	1037.1 (40.8)	904.3 (22.0)**	830.8 (26.4)**
triglycerides (mg/dL)	69.0 (3.4)	74.6 (3.5)	59.0 (2.6)*	66.5 (3.2)
cholesterol (mg/dL)	138.6 (5.8)**	198.2 (5.9)	207.2 (4.1)	181.8 (4.3)
ALT (U/L)	15.9 (2.2)	20.7 (1.2)	16.8 (1.2)	16.8 (2.0)
free FAs (mEq/L)	0.97 (0.1)	0.99 (0.10)	0.86 (0.09)	0.80 (0.10)
lactate dehydrogenase (u/L)	193.3 (12.5)	215.1 (24.9)	184.4 (18.2)	182.2 (17.4)
fasting Glucose	244 (15)*	307 (8)	171 (8)**	235 (7)**

[a]All data are presented as mean (SEM). Statistical significance determined using *t*-test versus HFD, * < 0.05, ** < 0.01. Nine to 10 animals per experimental group.

HCl provided the HCl salt of the carboxylic acid intermediate **6** which was then coupled to cyclobutylamine using the HBTU coupling reagent to provide the free base of compound **13**. Finally, treatment of 2 M HCl in methanol gave the hydrochloride salt of **13**.

Intermediate **1** (**36**) was synthesized as shown in Scheme 2.[11] 2,6-Dimethoxy acetophenone **40** was condensed with diethyl oxalate to afford the sodium salt of diketone **41** in quantitative yield. Reaction of **41** with cyclopentylhydrazine trifluoroacetate in refluxing glacial acetic acid provided 1,5-pyrazoles **42a** and 1,3-pyrazoles **42b** in a ratio of 4:1. Hydrolysis of ethyl ester **42a** to acid **36** was achieved using lithium hydroxide monohydrate.

Synthesis of intermediate 2 (**47**) was achieved as described in Scheme 3 using reported methods.[46] 3-Benzyloxy-1-propanol **43** was oxidized to **44** using Dess−Martin periodinane, which then underwent Horner−Wadsworth-Emmons reaction with *tert*-butyl diethylphosphonoacetate to provide alkene **45**. BuLi-facilitated addition of (*S*)-*N*-benzyl-*N*-α-methyl-benzylamine to **45** gave intermediate **46** which was then hydrogenated using 10% Pd/C catalyst to provide the intermediate 2 (**47**).

Target compounds **4**−**11** and **12**−**18** were synthesized, as shown in Scheme 4. Reductive amination of aldehyde **38** with cycloalkyl amines gave the corresponding *tert*-butyl ester intermediates. Deprotection of *tert*-butyl ester intermediates with 4 M HCl provided the HCl salt of carboxylic acids **4**−**11** which were then coupled to cyclobutylamine using the HBTU coupling reagent to give the free base of compounds **12**−**18**. Finally, treatment of the free base with 2 M HCl in methanol gave the hydrochloride salts of **12**−**18**.

Target compound **34** and diverse amide analogues **20**−**33** were synthesized as described in Scheme 5. Starting compound **6** was converted to the amide **48** using Boc_2O and $(NH_4)_2CO_3$. Amide **48** was treated with DMF−DMA to obtain the reactive aldehyde intermediate which was further treated with hydrazine hydrate to provide the target compound **34**. HBTU-facilitated coupling of **6** with diverse alkyl amines provided the amide analogues **20**−**33**.

Scheme 6 describes the synthesis of target compound **35**. Starting compound **39** was first converted to the methyl ester **49** which was then treated with hydrazine hydrate to provide the hydrazide intermediate **50**. Hydrazide **50** was then treated with triethyl orthoformate to provide the target compound **35**.

Efficacy Study of 13 in the DIO Mouse Model. The DIO model of metabolic syndrome is a well-accepted model of this disorder and has a high degree of correlation to clinical outcome in humans. Twice daily administration of the compound **13** at two different doses—5 and 15 mg/kg for 28 days—led to improved metabolic parameters (Table 6) in mice maintained on a 60% fat-containing diet (HFD) compared to animals receiving vehicle alone. Animals on 10% fat diet (ND) served as baseline controls for this experiment. Compared to mice on HFD alone, several biomarkers associated with metabolic syndrome showed statistically significant improvement including fructosamine levels (the level of fructosamine in the blood is a reflection of glucose levels over the previous 2−3 weeks similar to hemoglobin A1c), total fat pad weights, and triglycerides. Cholesterol, ALT, lactate dehydrogenase (LDH), and free FA concentrations in plasma trended lower upon treatment as well. The most pronounced effects were noticed at the higher dose, including reduced food consumption, suggesting a central role of APJ in regulation of feeding and associated metabolic processes. However, certain benefits such as fasting glucose levels were noted at the lower dose groups in the absence of a pronounced effect on body weight presumably through the activation of peripheral APJ receptors in agreement with the past literature.[47,48] The oral GTT data recorded on day 28 indicated significant blunting of circulating glucose levels in fasted animals (Figure 3). Degree of liver steatosis was vastly reduced in animals treated with **13** in a dose-dependent fashion with minimum fat deposition noted at the high dose group (Figure 3). Taken together, these very promising studies firmly establish a role of apelin receptor agonists in the treatment of DIO and metabolic syndrome.

CONCLUSIONS

Systematic modification at the amino acid side chain of **2** and **3** and at the carboxylic acid end of **6** led to compound **13** with favorable agonist potency, HLM stability, and PK profile in rodents. At first, compounds with substituted alkyl/cycloalkyl amines replacing the cyclohexyl moiety in **2** were synthesized and evaluated to gain an understanding of receptor tolerances and their effects on potency and efficacy. Among these, compounds with five- (**5**) or seven-membered (**11**) heterocyclic rings (pyrrolidine and azepane) were tolerated well and exhibited comparable or enhanced agonist potency relative to compound **2**. In contrast, six-membered cyclic piperidine derivatives (**6**, **7**, **8**, and **9**) exhibited reduced receptor tolerance and variable agonist potencies. Several compounds among **4**−**11** exhibited weak activity in the β-arrestin recruitment assay suggesting the possibility of low receptor internalization and desensitization with these analogues. Furthermore, compounds **12**−**18** with diverse cycloamine substitutions at the amino acid

https://dx.doi.org/10.1021/acs.jmedchem.0c01448
J. Med. Chem. 2021, 64, 3006−3025

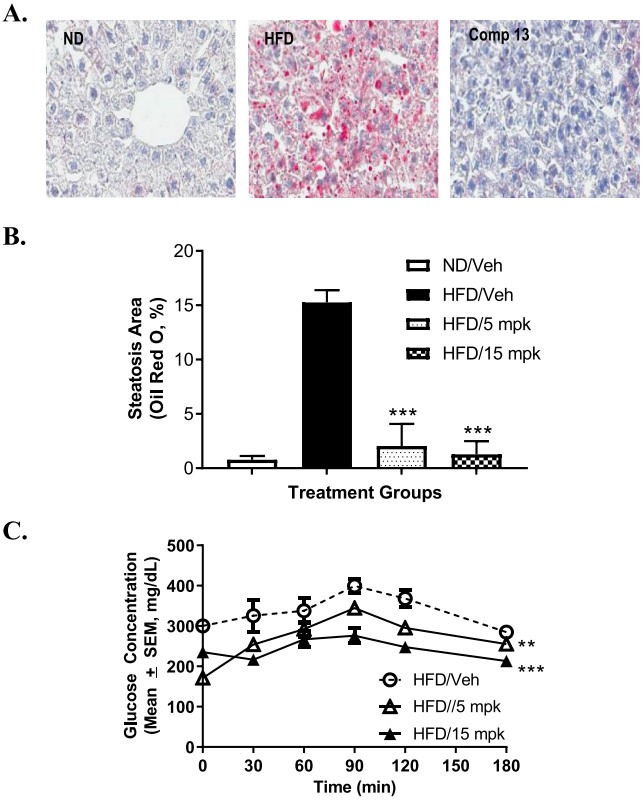

Figure 3. Treatment with **13** improved glucose tolerance and reduced hepatic steatosis. (A) Both macro- and microvesicular steatosis of the liver were reduced in mice receiving **13** as determined using Oil Red O staining. The representative image is taken from animals receiving 15 mg/kg dose of **13** along with ND and HFD controls receiving vehicle only. (B) Liver steatosis is decreased by **13** as determined by quantifying Oil Red O-positive staining in liver samples. Statistical significance indicated ($p < 0.01$, ** and $p < 0.001$, ***) following ANOVA with post hoc Dunnett test vs HFD group. (C) Oral GTT testing on day 28 indicated that treatment with **13** reduced fasting glucose levels and improved glucose utilization in a dose-dependent manner. Dose effects are significant for both groups ($p < 0.01$, ** and $p < 0.001$, ***) over time compared to HFD as assessed using ANOVA with a post hoc Dunnett test.

end of **3** were evaluated to examine if these substitutions enhanced potency. Interestingly, six-membered piperidine **13** (~13-fold), 2,6-dimethyl-substituted piperidine **16** (~65-fold), 7-azabicyclo [2.2.1] heptane **17** (21-fold), and seven-membered azepane cyclobutylamide **18** (~23-fold) substitutions significantly enhanced potency compared to their carboxylic acid precursors indicating enhanced receptor interaction with the addition of the cyclobutylamide group. Among these, compound **13** with a piperidine moiety had the most favorable HLM stability ($T_{1/2}$ = 62 min) and clearance (CL_{INT} = 20 mL/min/kg). Compounds **13**, **16**, and **18** also recruited β-arrestin with an EC_{50} value < 1 μM. To further improve potency and stability, the cyclobutyl end of **13** was replaced with diverse polar and nonpolar substituted amides and nonamide moieties. The compound with thiazolylamide (**29**) was the most potent (~167-fold compared to **13**), however it was surprisingly metabolized faster than **13**. Similarly, compounds with 1,1-difluorocyclobutanamide (**20**, 18-fold) and *N*-methylthiazolamide (**30**, 33-fold) were significantly more potent than **13** but were metabolized more rapidly than **13** suggesting emergence of additional liabilities due to these substitutions. Ultimately, compound **13** was deemed suitable for *in vivo* efficacy study based on the favorable agonist potency, HLM stability, *in vitro* ADMET, and PK properties. Upon evaluation in the mouse model of DIO, compound **13** exhibited significant weight loss, improved glucose utilization, and reduced liver steatosis and associated biomarkers.

In conclusion, we have identified a small-molecule agonist of the apelin receptor that is suitable for *in vivo* investigation in DIO and possibly in animal models of other diseases modulated by the apelin receptor. Favorable *in vivo* efficacy demonstrated by compound **13** in DIO firmly establishes a role of apelin receptor agonists in the treatment of DIO and metabolic syndrome.

EXPERIMENTAL SECTION

Reagents and starting materials were obtained from commercial suppliers and were used without purification. Reactions were conducted under a N_2 atmosphere using oven-dried glassware. All solvents and chemicals used were reagent grade. Anhydrous tetrahydrofuran (THF), dichloromethane (DCM), and *N*,*N*-dimethylformamide (DMF) were purchased from Fisher Scientific and used as such. Flash column chromatography was carried out using a Teledyne ISCO Combiflash Rf system and Redisep Rf gold prepacked HP silica columns. Purity and characterization of compounds were established using a combination of HPLC, TLC, and NMR analytical techniques described below. ^{1}H NMR spectra were recorded on a Bruker AVANCE DPX300 (300 MHz) or Variance 200 (200 MHz) spectrometer using $CHCl_3$-*d*, MeOH-d_4, and DMSO-d_6 with tetramethylsilane (TMS) (0.00 ppm) as the internal reference. Chemical shifts are reported in ppm relative to the solvent signal, and coupling constant (*J*) values are reported in Hertz (Hz). Thin-layer chromatography (TLC) was performed on precoated silica gel GF Uniplates from Analtech and spots were visualized with UV light or I_2 detection or phosphomolybdic acid stain. Low-resolution mass spectra were obtained using a Waters Alliance HT/Micromass ZQ system (ESI). Analytical HPLC was performed on a Waters 2695 Separation Module equipped with a Waters 2996 photodiode array detector and a Phenomenex Synergi 4 μm Hydro-RP 80A C18 250 × 4.6 mm column using a flow rate of 1 mL/min starting with 1 min at 5% solvent B, followed by a 15 min gradient of 5−95% solvent B, followed by 9 min at 95% solvent B (solvent A, water with 0.1% TFA; solvent B, acetonitrile with 0.1% TFA and 5% water); absorbance was monitored at 220 and 280 nm. Purity of the target compounds was determined to be ≥95% by HPLC. Optical rotations were measured on an Auto Pol IV automatic polarimeter at the sodium D line. Chemical names were generated using ChemDraw Ultra (CambridgeSoft, version 10.0).

Scheme 1: Synthesis of (*S*)-*N*-(1-(Cyclobutylamino)-1-oxo-5-(piperidin-1-yl)pentan-3-yl)-1-cyclopentyl-5-(2,6-dimethoxyphenyl)-1*H*-pyrazole-3-carboxamide Hydrochloride (13). *tert-Butyl-(S)-3-(5-(2,6-dimethoxyphenyl)-1-cyclopentyl-1H-pyrazole-3-carboxamido)-5-hydroxypentanoate (**37**).* To a solution of (*S*)-*tert*-butyl 3-amino-5-hydroxypentanoate **47** (16 g, 0.084 mol) and 5-(2,6-dimethoxyphenyl)-1-cyclopentyl-1*H*-pyrazole-3-carboxylic acid **36** (26.7 g, 0.084 mol) in MeCN (400 mL) were added HBTU (64 g, 0.169 mol) followed by the dropwise addition of triethylamine (35.3 mL, 0.253 mol) at room temperature. After stirring at room temperature for 16 h, the reaction mixture was quenched using saturated aqueous sodium bicarbonate (250 mL). The layers were separated, and the aqueous layer was extracted with EtOAc (3 × 200 mL). The combined organic layers were dried with Na_2SO_4, filtered, and concentrated in vacuo to give the crude product. The crude product was purified by silica gel flash column chromatography (0−100% EtOAc/hexanes containing 5% triethylamine) to give the purified title compound **37** as light-yellow foam (18.6 g, 45%). ^{1}H NMR ($CDCl_3$, 300 MHz): δ 1.49 (s, 9H), 1.51−1.75 (m, 4H), 1.84−1.98 (m, 4H), 1.99−2.16 (m, 2H), 2.47−2.59 (m, 1H), 2.62−2.77 (m, 1H), 3.63−3.71 (m, 2H), 3.73 (s, 3H), 3.75 (s, 3H), 4.23−4.33 (m, 1H), 4.55−4.67 (m, 1H), 6.63 (dd, *J* = 8.48, 1.70 Hz, 2H), 6.66−6.72 (m, 1H), 7.38

https://dx.doi.org/10.1021/acs.jmedchem.0c01448
J. Med. Chem. 2021, 64, 3006−3025

(t, J = 8.48 Hz, 1H), 7.68 (d, J = 9.61 Hz, 1H). MS (ESI) m/z: calcd for $C_{26}H_{37}N_3O_6$, 487.27 $[M]^+$; found, 488.7 $[M + H]^+$.

***tert*-Butyl (*S*)-3-(1-Cyclopentyl-5-(2,6-dimethoxyphenyl)-1*H*-pyrazole-3-carboxamido)-5-oxopentanoate (38).** *tert*-Butyl-(*S*)-3-(5-(2,6-dimethoxyphenyl)-1-cyclopentyl-1*H*-pyrazole-3-carboxamido)-5-hydroxypentanoate **37** (11.19 g, 22.95 mmol) was dissolved in DCM (saturated with water, 90 mL). Dess−Martin periodinate (20 g, 47.26 mmol) was added, and the reaction mixture was stirred at RT for 1 h, with the addition of 15 mL of DCM (saturated with water) every 15 min. Upon completion, the mixture was diluted with diethyl ether (400 mL). A mixture containing sodium thiosulfate (20 g) dissolved in saturated sodium bicarbonate (80 mL) and water (20 mL) was added. This mixture was stirred for 30 min at room temperature. The aqueous layer was extracted with ether, and the combined organic layers were washed with ice-cold saturated sodium bicarbonate solution (2 × 150 mL) and brine (150 mL). The mixture was dried (Na_2SO_4), filtered, and concentrated to yield 11.0 g (98%) of compound **38** as a tan solid which was used without further purification. ^{1}H NMR ($CDCl_3$, 300 MHz): δ 1.48 (s, 9H), 1.49−1.62 (m, 2H), 1.83−1.97 (m, 3H), 1.98−2.14 (m, 3H), 2.70 (d, J = 5.84 Hz, 2H), 2.78−3.01 (m, 2H), 3.73 (s, 6H), 4.26 (quin, J = 7.21 Hz, 1H), 4.82−4.94 (m, 1H), 6.62 (d, J = 8.48 Hz, 2H), 6.66 (s, 1H), 7.37 (t, J = 8.38 Hz, 1H), 7.53 (d, J = 9.23 Hz, 1H), 9.81 (s, 1H). MS (ESI) m/z: calcd for $C_{26}H_{35}N_3O_6$, 485.25 $[M]^+$; found, 486.7 $[M + H]^+$.

***tert*-Butyl (*S*)-3-(5-(2,6-Dimethoxyphenyl)-1-cyclopentyl-1*H*-pyrazole-3-carboxamido)-5-(piperidin-1-yl)pentanoate (39).** Crude *tert*-butyl (*S*)-3-(1-cyclopentyl-5-(2,6-dimethoxyphenyl)-1*H*-pyrazole-3-carboxamido)-5-oxopentanoate **38** (11.0 g, 22.61 mmol) was mixed with DCE (170 mL). To the solution, piperidine (2.8 mL, 28.3 mmol) and $NaBH(OAc)_3$ (9.9 g, 46.57 mmol) were added at RT. The mixture was stirred at RT for 16 h. The reaction mixture was then quenched with sat. $NaHCO_3$ and diluted with DCM. The organic layer was then washed with water and brine, dried with Na_2SO_4, and concentrated to give the crude product. The crude residue was purified by silica gel flash chromatography (0−30% DCM/MeOH/aq. NH_4OH (100:20:2)/DCM) to give the title compound **39** as white foam (7.74 g, 61%). ^{1}H NMR ($CDCl_3$, 300 MHz): δ 1.52−1.64 (m, 5H), 1.46 (s, 9H), 1.51−1.67 (m, 5H), 1.78−1.98 (m, 6H), 1.99−2.14 (m, 2H), 2.35−2.70 (m, 6H), 3.72 (s, 3H), 3.74 (s, 3H), 4.25 (quin, J = 7.63 Hz, 1H), 4.42−4.55 (m, 1H), 6.62 (d, J = 8.48 Hz, 2H), 6.67 (s, 1H), 7.32−7.40 (m, 1H), 7.69 (d, J = 8.67 Hz, 1H). MS (ESI) m/z: calcd for $C_{31}H_{46}N_4O_5$, 554.35 $[M]^+$; found, 556.1 $[M + H]^+$.

(*S*)-*N*-(1-(Cyclobutylamino)-1-oxo-5-(piperidin-1-yl)pentan-3-yl)-5-(2,6-dimethoxyphenyl)-1-cyclopentyl-1*H*-pyrazole-3-carboxamide Hydrochloride (13). *tert*-Butyl (*S*)-3-(5-(2,6-dimethoxyphenyl)-1-cyclopentyl-1*H*-pyrazole-3-carboxamido)-5-(piperidin-1-yl)pentanoate **39** (2.71 g, 4.88 mmol) was dissolved in anhydrous DCM (40 mL) and treated with 4 M HCl/dioxane (18.3 mL, 73.2 mmol); this mixture was stirred for 8 h at RT. Upon completion, the reaction mixture was concentrated and vacuum-dried overnight to obtain quantitative yield of (*S*)-3-(5-(2,6-dimethoxyphenyl)-1-cyclopentyl-1*H*-pyrazole-3-carboxamido)-5-(piperidin-1-yl)pentanoic acid **6** as a hydrochloride salt. MS (ESI) m/z: calcd for free base $C_{27}H_{38}N_4O_5$, 498.28 $[M]^+$; found, 499.52 $[M + H]^+$.

To a solution of crude (*S*)-3-(5-(2,6-dimethoxyphenyl)-1-cyclopentyl-1*H*-pyrazole-3-carboxamido)-5-(piperidin-1-yl)pentanoic acid hydrochloride **6** (16.6 g, 0.0258 mol) and cyclobutylamine (2.42 mL, 0.0283 mol) in MeCN (200 mL) were added triethylamine (17.95 mL, 0.129 mol) and HBTU (14.6 g, 0.0386 mol). After stirring at room temperature for 4 h, the reaction mixture was quenched using saturated aqueous sodium bicarbonate solution (100 mL). The aqueous layer was separated and extracted with EtOAc (3 × 100 mL). The combined organic layers were further washed with 50% concentrated NH_4OH/H_2O (2 × 50 mL), dried with Na_2SO_4, filtered, and concentrated in vacuo to give the crude product. The crude product was purified by silica gel flash column chromatography (0−30% DCM/MeOH/aq. NH_4OH (100:20:2)/DCM). Purified fractions were combined and concentrated. The residue was dissolved in DCM (200 mL), washed with 50% concentrated NH_4OH/H_2O (50 mL) and brine (50 mL), and dried with Na_2SO_4. Removal of the solvent in vacuo afforded the pure free base of **13** (12.31 g, 87%) as a white solid. ^{1}H NMR ($CDCl_3$, 300 MHz): δ 1.38−1.49 (m, 2H), 1.49−1.72 (m, 10H), 1.78−2.00 (m, 7H), 2.01−2.18 (m, 2H), 2.19−2.33 (m, 2H), 2.34−2.50 (m, 4H), 2.50−2.69 (m, 3H), 3.72 (s, 3H), 3.73 (s, 3H), 4.24 (quin, J = 7.63 Hz, 1H), 4.34−4.49 (m, 2H), 6.63 (d, J = 8.29 Hz, 2H), 6.67 (s, 1H), 7.01 (d, J = 8.67 Hz, 1H), 7.38 (t, J = 8.29 Hz, 1H), 8.09 (d, J = 8.29 Hz, 1H). MS (ESI) m/z: calcd for $C_{31}H_{45}N_5O_4$, 551.35 $[M]^+$; found, 552.8 $[M + H]^+$.

The free base of (*S*)-*N*-(1-(cyclobutylamino)-1-oxo-5-(piperidin-1-yl)pentan-3-yl)-5-(2,6-dimethoxyphenyl)-1-cyclopentyl-1*H*-pyrazole-3-carboxamide **13** (9.0 g, 16.68 mmol) was mixed with MeOH (100 mL) at 0 °C. To it was added 2 M HCl solution in ether (16.7 mL, 33.37 mmol) dropwise at 0 °C. The reaction mixture was warmed to room temperature and stirred for 30 min. MeOH was evaporated in vacuo and dried under high vacuum to remove all the excess HCl. To it was added ether, triturated, and filtered to obtain a white solid. The solid was dried under high vacuum for 16 h to give the hydrochloride salt of **13** (10.1 g). ^{1}H NMR (DMSO-d_6, 300 MHz): δ 1.46−1.69 (m, 4H), 1.69−1.79 (m, 4H), 1.79−2.05 (m, 9H), 2.07−2.18 (m, 2H), 2.43 (t, J = 8.85 Hz, 2H), 2.77−2.93 (m, 2H), 2.97−3.12 (m, 2H), 3.34−3.47 (m, 2H), 3.71 (s, 6H), 4.13−4.34 (m, 6H), 6.45 (s, 1H), 6.78 (d, J = 8.29 Hz, 2H), 7.44 (t, J = 8.38 Hz, 1H), 8.04 (d, J = 8.85 Hz, 1H), 8.32 (d, J = 7.54 Hz, 1H), 9.99 (br s, 1H). ^{13}C NMR (75 MHz, DMSO-d_6): δ 14.68, 21.35, 22.32, 24.01, 24.05, 28.38, 30.08, 30.19, 32.50, 43.83, 44.26, 51.82, 51.97, 53.54, 55.68, 59.42, 104.20, 106.71, 107.35, 131.46, 136.42, 144.82, 158.18, 158.21, 161.38, 168.83. MS (ESI) m/z: calcd for free base $C_{31}H_{45}N_5O_4$, 551.35 $[M]^+$; found, 552.8 $[M + H]^+$; $[\alpha]_D^{25}$ −23.56 (c 0.50, MeOH).

Synthesis of Intermediates. ***Intermediate 1.*** *Synthesis of 1-Cyclopentyl-5-(2,6-dimethoxyphenyl)-1H-pyrazole-3-carboxylic Acid. Ethyl 4-(2,6-Dimethoxyphenyl)-2,4-dioxobutanoate (**41**).* To a solution of sodium ethoxide (21% in EtOH) (5.4 mL, 14.37 mmol) was added dropwise a mixture of diethyl oxalate (1.85 mL, 13.690 mmol) and 2,6-dimethoxy acetophenone **40** (2.45 g, 13.690 mmol) in anhydrous ethanol (15 mL). The resultant mixture was stirred at RT for 30 min, upon which yellow suspension formed. The reaction mixture was heated to reflux for 4 h. The reaction mixture was cooled to room temperature. Ethanol was evaporated in vacuo. The resultant residue was triturated with diethyl ether (30 mL) and filtered to obtain a sodium salt of ethyl 4-(2,6-dimethoxyphenyl)-2,4-dioxobutanoate **41** as a yellow solid (4.0 g, 97%). MS (ESI) m/z: calcd for $C_{14}H_{16}O_6$, 280.09 $[M]^+$; found, 279.3 $[M - H]^-$.

*Ethyl 1-Cyclopentyl-5-(2,6-dimethoxyphenyl)-1H-pyrazole-3-carboxylate (**42a**).* Step 1: Preparation of cyclopentylhydrazine trifluoroacetate: cyclopentanone (2.0 g, 23.77 mmol) and *tert*-butyl carbazate (3.1 g, 23.77 mmol) in methanol (20 mL) were stirred at room temperature for 3 h. The solvent was evaporated, and the resulting solid was dried in vacuo to give a white solid of *tert*-butyl 2-cyclopentylidenehydrazinecarboxylate (4.6 g, 98%). Sodium cyanoborohydride (2.1 g, 34.06 mmol) was added portionwise to a mixture of *tert*-butyl 2-cyclopentylidenehydrazinecarboxylate (4.5 g, 22.697 mmol) in 75% of aqueous acetic acid (25 mL) at room temperature. The resultant solution was stirred for 3 h at room temperature. The reaction mixture was neutralized with 1 N NaOH and extracted with CH_2Cl_2 (3 × 30 mL). The organic layer was washed with saturated $NaHCO_3$, dried with Na_2SO_4, filtered, and evaporated to give *tert*-butyl 2-cyclopentylhydrazinecarboxylate as oil (4.4 g, 97%). ^{1}H NMR ($CDCl_3$, 300 MHz): δ 1.40−1.55 (m, 4H), 1.46 (s, 9H), 1.63−1.75 (m, 4H), 3.45−3.58 (m, 1H). MS (ESI) m/z: calcd for $C_{10}H_{20}N_2O_2$, 200.15 $[M]^+$; found, 223.3 $[M + Na]^+$.

Trifluoroacetic acid (24 mL) was added dropwise to a solution of the *tert*-butyl 2-cyclopentylhydrazinecarboxylate (4.4 g, 21.97 mmol) in CH_2Cl_2 (24 mL). The reaction mixture was stirred at room temperature for 2.5 h. The solvent was evaporated to give cyclopentylhydrazine trifluoroacetate as colorless oil in quantitative yield. ^{1}H NMR ($CDCl_3$, 300 MHz): δ 1.58−1.70 (m, 2H), 1.72−1.92 (m, 4H), 1.95−2.09 (m, 2H), 3.60−3.78 (m, 1H). MS (ESI) m/z: calcd for $C_5H_{12}N_2$, 100.10 $[M]^+$; found, 101.2 $[M + H]^+$.

Step 2: Preparation of ethyl 1-cyclopentyl-5-(2,6-dimethoxyphenyl)-1*H*-pyrazole-3-carboxylate (**42a**): Sodium salt of ethyl 4-(2,6-

https://dx.doi.org/10.1021/acs.jmedchem.0c01448
J. Med. Chem. 2021, 64, 3006−3025

dimethoxyphenyl)-2,4-dioxobutanoate (**41**) (1.2 g, 3.96 mmol) and cyclopentylhydrazine trifluoroacetate (1.3 g, 5.95 mmol) were mixed with glacial acetic acid (25 mL) and conc. HCl (0.6 mL). The reaction mixture was heated to reflux for 3 h. After cooling, the reaction mixture was poured into water (50 mL). The aqueous layer was extracted with DCM (3 × 30 mL). The combined DCM layer was washed with saturated aqueous $NaHCO_3$. The organic layer was then washed with saturated brine and then dried over Na_2SO_4, followed by filtration. The solvent was evaporated in vacuo. The residue was purified by silica gel flash chromatography (0−40% EtOAc/Hex) to give N_1-substituted title compound **42a** (1.0 g, 73%, major product) as a light-yellow solid and less polar N_2-substituted **42b**, 2-cyclopentyl-5-(2,6-dimethoxyphenyl)-1*H*-pyrazole-3-carboxylate as colorless oil (50 mg, 5%).

*Ethyl 1-Cyclopentyl-5-(2,6-dimethoxyphenyl)-1H-pyrazole-3-carboxylate (**42a**).* ^{1}H NMR ($CDCl_3$, 300 MHz): δ 1.38 (t, J = 7.2 Hz, 3H), 1.44−1.57 (m, 2H), 1.84−1.98 (m, 4H), 2.08−2.26 (m, 2H), 3.74 (s, 6H), 4.21−4.31 (m, 1H), 4.39 (q, J = 6.9 Hz, 2H), 6.63 (d, J = 8.3 Hz, 2H), 6.69 (s, 1H), 7.38 (t, J = 8.48 Hz, 1H). MS (ESI) m/z: calcd for $C_{19}H_{24}N_2O_4$, 344.17 $[M]^+$; found, 345.0 $[M + H]^+$.

*Ethyl 2-Cyclopentyl-5-(2,6-dimethoxyphenyl)-1H-pyrazole-3-carboxylate (**42b**).* ^{1}H NMR ($CDCl_3$, 300 MHz): δ 1.36 (t, J = 7.2 Hz, 3H), 1.62−1.74 (m, 2H), 1.85−1.98 (m, 2H), 2.08−2.26 (m, 4H) 3.77 (s, 6H), 4.33 (q, J = 7.16 Hz, 2H), 5.68 (quin, J = 7.49 Hz, 1H), 6.62 (d, J = 8.48 Hz, 2H), 6.91 (s, 1H), 7.27 (t, J = 8.48 Hz, 1H). MS (ESI) m/z: calcd for $C_{19}H_{24}N_2O_4$, 344.17 $[M]^+$; found, 345.3 $[M + H]^+$.

*1-Cyclopentyl-5-(2,6-dimethoxyphenyl)-1H-pyrazole-3-carboxylic Acid (**36**).* Lithium hydroxide monohydrate (440 mg, 10.452 mmol) in 2.5 mL of water was added to a solution of ethyl 1-cyclopentyl-5-(2,6-dimethoxyphenyl)-1*H*-pyrazole-3-carboxylate (**42a**) (1.2 mg, 3.484 mmol) in MeOH (11 mL) and THF (2.5 mL). The mixture was stirred at RT for 18 h. The reaction mixture was concentrated to about half the volume and then extracted with ether (2 × 15 mL). The aqueous layer was acidified with 1 N HCl and extracted with CH_2Cl_2 (3 × 25 mL). The combined organic layers were washed with water and brine and then dried with Na_2SO_4. The solvent was evaporated in vacuo to give the title compound as a white solid (1 g, 98% yield). ^{1}H NMR ($CDCl_3$, 300 MHz): δ 1.48−1.64 (m, 2H), 1.84−2.02 (m, 4H), 2.03−2.20 (m, 2H), 3.75 (s, 6H), 4.30 (quin, J = 7.4 Hz, 1H), 6.64 (d, J = 8.3 Hz, 2H), 6.76 (s, 1H), 7.40 (t, J = 8.3 Hz, 1H). MS (ESI) m/z: calcd for $C_{17}H_{20}N_2O_4$, 316.14 $[M]^+$; found, 317.2 $[M + H]^+$.

***Intermediate 2**. Synthesis of (S)-tert-Butyl 3-Amino-5-hydroxypentanoate (**47**). 3-(Benzyloxy)propanal (**44**).* To a solution of commercially available 3-benzyloxy-1-propanol **43** (160 g, 0.96 mol) in CH_2Cl_2 (2000 mL) at 0 °C was added Dess−Martin periodinane (450 g, 1.06 mol) in 50 g portions, and the reaction mixture was stirred at RT for 3 h. To the reaction mixture was added solution of 20% $Na_2S_2O_3$ solution (1 L) and stirred for 15 min. The reaction mixture was poured into a separating funnel containing Et_2O (2 L). The organic phase was washed with 1:1:1 20% $Na_2S_2O_3$ solution/sat. $NaHCO_3$/H_2O (750 mL) and brine (250 mL). The organic phase was concentrated to give a crude solid which was filtered over Celite and washed with THF. The filtrate was concentrated and dried to give 155 g (98%) of 3-(benzyloxy)propanal **44** as a pale-yellow liquid. ^{1}H NMR (DMSO-d_6, 300 MHz): δ 2.70 (t, J = 6.2 Hz, 2H), 3.70 (t, J = 6.2 Hz, 2H), 4.55 (s, 2H), 7.25−7.40 (m, 5H), 9.80 (s, 1H).

*(E)-tert-Butyl 5-(Benzyloxy)pent-2-enoate (**45**).* To a stirred solution of *tert*-butyl diethylphosphonoacetate (286 g, 1.13 mol) in THF (1400 mL) at −78 °C was added *n*-BuLi (2.5 M in hexanes) (453 mL, 1.13 mol) using a dropping funnel over 40 min. After stirring for 30 min at −78 °C, a solution of 3-(benzyloxy)propanal **44** (42.3 g, 0.945 mol) in THF (600 mL) also cooled at −78 °C was transferred via cannula. The resulting solution was stirred at −78 °C for 40 min before being allowed to warm at RT and then stirred for 1 h. The solution was subsequently cooled to −78 °C and quenched with saturated aqueous NH_4Cl (250 mL). The reaction mixture was brought to RT. The layers were separated, the aqueous layer was extracted in EtOAc (500 mL), the combined organics were dried over Na_2SO_4 and filtered, and the solvent was evaporated in vacuo to give the crude residue. The crude product was purified by silica gel flash chromatography (0−5% of EtOAc in hexanes), and the fractions containing the product were pooled and evaporated to obtain 152 g (61%) of (*E*)-*tert*-butyl 5-(benzyloxy)pent-2-enoate **45** as a colorless liquid. ^{1}H NMR (DMSO-d_6, 300 MHz): δ 1.45 (s, 9H), 2.40−2.60 (m, 2H), 3.55 (t, J = 6.8 Hz, 2H), 4.50 (s, 2H), 5.80 (s, 1H), 6.80−6.95 (m, 1H), 7.30−7.40 (m, 5H). MS (ESI) m/z: calcd for $C_{16}H_{22}O_3$, 262.16 $[M]^+$; found, 263.1 $[M + H]^+$

*(S)-tert-Butyl 3-(Benzyl((S)-1-phenylethyl)amino)-5-(benzyloxy)-pentanoate (**46**).* To a stirred solution of (*S*)-*N*-benzyl-*N*-α-methybenzylamine (150 g, 0.710 mol) in THF (600 mL) at −78 °C was added *n*-BuLi (2.5 M in hexanes) (285 mL, 0.710 mol) using a dropping funnel. After 30 min, a solution of (*E*)-*tert*-butyl 5-(benzyloxy)pent-2-enoate **45** (152 g, 0.546 mol) in THF (200 mL) also at −78 °C was transferred via cannula. The resulting solution was stirred at −78 °C for 3 h, warmed to −10 °C, and quenched with 20% citric acid solution (900 mL). The organic phase was separated, washed with brine (500 mL), and dried with Na_2SO_4, and the solvent was removed in vacuo to give the crude product. The crude product was purified by silica gel flash chromatography (0−4% of EtOAc in hexanes), and the fractions containing the product were pooled and evaporated to obtain 155 g (60%) of (*S*)-*tert*-butyl 3-(benzyl((*S*)-1-phenylethyl)amino)-5-(benzyloxy)pentanoate **46** as a pale-yellow liquid. ^{1}H NMR (DMSO-d_6, 300 MHz): δ 1.40−1.80 (m, 12H), 1.60−1.80 (m, 2H), 1.85−1.90 (m, 2H), 3.40−3.80 (m, 6H), 4.52−4.60 (m, 2H), 7.15−7.40 (m, 15H). MS (ESI) m/z: calcd for $C_{31}H_{39}NO_3$, 473.29 $[M]^+$; found, 474.3 $[M + H]^+$; $[\alpha]_D^{25}$ +6.47 (*c* 0.850, MeOH).

*(S)-tert-Butyl 3-Amino-5-hydroxypentanoate (**47**).* (*S*)-*tert*-Butyl 3-(benzyl((*S*)-1-phenylethyl)amino)-5-(benzyloxy)pentanoate **46** (65.4 g, 138 mmol) was dissolved in 20% acetic acid in EtOH (550 mL) and to it was added 10% Pd/C (10.5 g). The mixture was hydrogenated in a sealed vessel at 50 psi for 48 h. The catalyst was removed by filtration through celite, and the solvent was evaporated to obtain the crude product as oil. The crude product was basified at 0 °C with NH_4OH solution (35 mL) to pH 9.0. This crude mixture was loaded onto a column and purified by silica gel flash chromatography (0−40% and 40−60% of DCM/MeOH/aq. NH_4OH (100:20:2)/DCM) to give the 23 g (88%) of (*S*)-*tert*-butyl 3-amino-5-hydroxypentanoate **47** as colorless oil. ^{1}H NMR (DMSO-d_6, 300 MHz): δ 1.40 (s, 9H), 1.55−1.65 (m, 2H), 2.20−2.40 (m, 2H), 2.50 (br, 2H), 3.25−3.40 (m, 1H), 3.75−3.85 (m, 2H). MS (ESI) m/z: calcd for $C_9H_{19}NO_3$, 189.14 $[M]^+$; found, 190.0 $[M + H]^+$; $[\alpha]_D^{25}$ −4.21 (*c* 0.285, MeOH).

*(S)-3-(1-Cyclopentyl-5-(2,6-dimethoxyphenyl)-1H-pyrazole-3-carboxamido)-5-(diethylamino)pentanoic Acid Hydrochloride (**4**).* Crude (*S*)-*tert*-butyl (*S*)-3-(5-(2,6-dimethoxyphenyl)-1-cyclopentyl-1*H*-pyrazole-3-carboxamido)-5-oxopentanoate **38** (60 mg, 0.123 mmol) was mixed with DCE (5 mL). To the mixture was added diethylamine (11 mg, 0.148 mmol) and $NaBH(OAc)_3$ (52 mg, 0.246 mmol) at RT. The reaction mixture was stirred at room temperature for 16 h. The reaction mixture was then quenched with saturated $NaHCO_3$, diluted with DCM (50 mL), and washed with water followed by brine. The organic layer was separated, dried with Na_2SO_4, filtered, and concentrated to give the crude product. The crude residue was purified by silica gel flash chromatography (0−30% DCM/MeOH/aq. NH_4OH (100:20:2)/DCM) to give *tert*-butyl (*S*)-3-(1-cyclopentyl-5-(2,6-dimethoxyphenyl)-1*H*-pyrazole-3-carboxamido)-5-(diethylamino)-pentanoate as white foam (65 mg, 73%).

4 M HCl in dioxane (0.2 mL) was added to *tert*-butyl (*S*)-3-(1-cyclopentyl-5-(2,6-dimethoxyphenyl)-1*H*-pyrazole-3-carboxamido)-5-(diethylamino)pentanoate (53 mg, 0.097 mmol) in 3 mL of DCM. The reaction mixture was stirred at RT for 24 h, and the solvent was evaporated. The solid residue was triturated with ethyl ether and filtered to obtain 45 mg (94%) of the title compound **4** as a white solid. ^{1}H NMR (MeOH-d_4, 300 MHz): δ 1.35 (t, J = 7.25 Hz, 6H), 1.53−1.69 (m, 2H), 1.83−2.25 (m, 8H), 2.79 (d, J = 6.2 Hz, 2H), 3.12−3.29 (m, 4H), 3.46−3.59 (m, 1H), 3.68 (m, 3H), 3.69−3.65 (m, 1H), 3.72−3.77 (m, 2H), 3.76 (s, 3H), 4.24−4.40 (m, 1H), 4.41−4.58 (m, 1H), 6.56 (s, 1H), 6.77 (d, J = 8.5 Hz, 2H), 7.46 (t, J = 8.4 Hz, 1H). MS (ESI) m/z:

https://dx.doi.org/10.1021/acs.jmedchem.0c01448
J. Med. Chem. 2021, 64, 3006−3025

calcd for free base $C_{26}H_{38}N_4O_5$, 486.28 $[M]^+$; found, 487.6 $[M + H]^+$; $[\alpha]_D^{25}$ −24.88 (*c* 0.225, MeOH).

*(S)-3-(1-Cyclopentyl-5-(2,6-dimethoxyphenyl)-1H-pyrazole-3-carboxamido)-5-(pyrrolidin-1-yl)pentanoic Acid Hydrochloride (**5**).* Compound **5** (60 mg) was synthesized using *tert*-butyl (*S*)-3-(5-(2,6-dimethoxyphenyl)-1-cyclopentyl-1*H*-pyrazole-3-carboxamido)-5-oxopentanoate **38** (60 mg, 0.123 mmol) and pyrrolidine (11 mg, 0.148 mmol) as described in procedure **4**. 92% yield; white solid; ^{1}H NMR (MeOH-d_4, 300 MHz): δ 1.51−1.69 (m, 2H), 1.83−1.99 (m, 4H), 1.99−2.26 (m, 7H), 2.78 (d, *J* = 6.4 Hz, 2H), 3.02−3.18 (m, 1H), 3.21−3.35 (m, 3H), 3.45−3.57 (m, 1H), 3.62−3.71 (m, 4H), 3.76 (s, 6H), 4.26−4.37 (m, 1H), 4.47−4.59 (s, 1H), 6.57 (s, 1H), 6.77 (d, *J* = 8.5 Hz, 2H), 7.46 (t, *J* = 8.4 Hz, 1H). MS (ESI) *m*/*z*: calcd for free base $C_{26}H_{36}N_4O_5$, 484.27 $[M]^+$; found, 485.1 $[M + H]^+$. $[\alpha]_D^{25}$ −26.15 (*c* 0.260, MeOH).

*(S)-3-(1-Cyclopentyl-5-(2,6-dimethoxyphenyl)-1H-pyrazole-3-carboxamido)-5-(piperidin-1-yl)pentanoic Acid Hydrochloride (**6**).* Compound **6** (37 mg) was synthesized using *tert*-butyl (*S*)-3-(5-(2,6-dimethoxyphenyl)-1-cyclopentyl-1*H*-pyrazole-3-carboxamido)-5-oxopentanoate **38** (42 mg, 0.086 mmol) and piperidine (10 mg, 0.095 mmol) as described in procedure **4**. 96% yield; off-white solid; ^{1}H NMR ($CDCl_3$, 300 MHz): δ 1.37−1.63 (m, 3H), 1.80−1.98 (m, 8H), 1.98−2.12 (m, 2H), 2.13−2.37 (m, 2H), 2.62−2.78 (m, 2H), 2.82 (d, *J* = 8.5 Hz, 2H), 3.11−3.28 (m, 2H), 3.54−3.71 (m, 3H), 3.76 (s, 3H), 3.74 (s, 3H), 4.21−4.35 (m, 1H), 4.36−4.55 (m, 1H), 6.64 (d, *J* = 8.67 Hz, 3H), 7.40 (t, *J* = 8.5 Hz, 1H), 7.95 (d, *J* = 9.0 Hz, 1H), 10.01 (br s, 1H). MS (ESI) *m*/*z*: calcd for free base $C_{27}H_{38}N_4O_5$, 498.28 $[M]^+$; found, 499.8 $[M + H]^+$; $[\alpha]_D^{25}$ −36.00 (*c* 0.100, MeOH).

*(S)-3-(1-Cyclopentyl-5-(2,6-dimethoxyphenyl)-1H-pyrazole-3-carboxamido)-5-morpholinopentanoic Acid Hydrochloride (**7**).* Compound **7** (50 mg) was synthesized using *tert*-butyl (*S*)-3-(5-(2,6-dimethoxyphenyl)-1-cyclopentyl-1*H*-pyrazole-3-carboxamido)-5-oxopentanoate **38** (60 mg, 0.123 mmol) and morpholine (13 mg, 0.148 mmol) as described in procedure **4**. 94% yield; white solid; ^{1}H NMR (MeOH-d_4, 300 MHz): δ 1.53−1.69 (m, 3H), 1.85−2.00 (m, 5H), 2.00−2.14 (m, 2H), 2.16−2.30 (m, 1H), 2.80 (d, *J* = 6.4 Hz, 2H), 3.11−3.29 (m, 5H), 3.65−3.69 (m, 4H), 3.76 (s, 6H), 3.83−4.08 (m, 3H), 4.24−4.41 (m, 1H), 4.43−4.59 (m, 1H), 6.57 (s, 1H), 6.77 (d, *J* = 8.5 Hz, 1H), 7.46 (t, *J* = 8.5 Hz, 1H). MS (ESI) *m*/*z*: calcd for free base $C_{26}H_{36}N_4O_6$, 500.26 $[M]^+$; found, 501.9 $[M + H]^+$; $[\alpha]_D^{25}$ −38.46 (c 0.065, MeOH).

*(S)-3-(1-Cyclopentyl-5-(2,6-dimethoxyphenyl)-1H-pyrazole-3-carboxamido)-5-(4-methylpiperazin-1-yl)pentanoic Acid Dihydrochloride (**8**).* Compound **8** (40 mg) was synthesized using *tert*-butyl (*S*)-3-(5-(2,6-dimethoxyphenyl)-1-cyclopentyl-1*H*-pyrazole-3-carboxamido)-5-oxopentanoate **38** (60 mg, 0.123 mmol) and 1-methylpiperazine (15 mg, 0.148 mmol) as described in procedure **4**. 95% yield; white solid; ^{1}H NMR (MeOH-d_4, 300 MHz): δ 1.52−1.68 (m, 2H), 2.10−1.83 (m, 6H), 2.09−2.32 (m, 2H), 2.82 (d, *J* = 6.4 Hz, 2H), 3.06 (s, 3H), 3.41 (t, *J* = 7.0 Hz, 2H), 3.48−3.96 (m, 4H), 3.63−3.71 (m, 5H), 3.76 (s, 6H), 4.26−4.37 (m, 1H), 4.47−4.59 (m, 1H), 6.59 (s, 1H), 6.77 (d, *J* = 8.5 Hz, 2H), 7.46 (t, *J* = 8.4 Hz, 1H). MS (ESI) *m*/*z*: calcd for free base $C_{27}H_{39}N_5O_5$, 513.30 $[M]^+$; found, 514.8 $[M + H]^+$; $[\alpha]_D^{25}$ −24.31 (c 0.255, MeOH).

*(3S)-3-(1-Cyclopentyl-5-(2,6-dimethoxyphenyl)-1H-pyrazole-3-carboxamido)-5-(2,6-dimethylpiperidin-1-yl)pentanoic Acid Hydrochloride (**9**).* Compound **9** (26 mg) was synthesized using *tert*-butyl (*S*)-3-(5-(2,6-dimethoxyphenyl)-1-cyclopentyl-1*H*-pyrazole-3-carboxamido)-5-oxopentanoate **38** (60 mg, 0.123 mmol) and 2,6-dimethylpiperidine (17 mg, 0.148 mmol) as described in procedure **4**. 90% yield; white solid; ^{1}H NMR (MeOH-d_4, 300 MHz): δ 1.28−1.50 (m, 6H), 1.51−1.82 (m, 5H), 1.82−2.30 (m, 9H), 2.72 (d, *J* = 6.4 Hz, 4H), 3.35−3.49 (m, 3H), 3.63−3.71 (m, 2H), 3.76 (s, 6H), 4.26−4.39 (m, 1H), 4.40−4.54 (m, 1H), 6.46−6.62 (m, 1H), 6.77 (d, *J* = 8.5 Hz, 2H), 7.46 (t, *J* = 8.3 Hz, 1H). MS (ESI) *m*/*z*: calcd for free base $C_{29}H_{42}N_4O_5$, 526.32 $[M]^+$; found, 527.7 $[M + H]^+$.

*(S)-5-(7-Azabicyclo[2.2.1]heptan-7-yl)-3-(1-cyclopentyl-5-(2,6-dimethoxyphenyl)-1H-pyrazole-3-carboxamido)pentanoic Acid Hydrochloride (**10**).* Compound **10** (60 mg) was synthesized using *tert*-butyl (*S*)-3-(5-(2,6-dimethoxyphenyl)-1-cyclopentyl-1*H*-pyrazole-3-carboxamido)-5-oxopentanoate **38** (60 mg, 0.123 mmol) and 7-azabicyclo[2.2.1]heptane (15 mg, 0.148 mmol) as described in procedure **4**. 83% yield; white solid; ^{1}H NMR (MeOH-d_4, 300 MHz): δ 1.52−1.69 (m, 2H), 1.78−2.00 (m, 7H), 2.00−2.28 (m, 6H), 2.80 (d, *J* = 6.4 Hz, 2H), 3.14−3.23 (m, 2H), 3.46−3.56 (q, *J* = 7.0 Hz, 2H), 3.64−3.71 (m, 3H), 3.76 (s, 6H), 4.13−4.19 (br s, 1H), 4.20−4.26 (m, 1H), 4.28−4.40 (m, 1H), 4.45−4.59 (m, 1H), 6.57 (s, 1H), 6.77 (d, *J* = 8.5 Hz, 2H), 7.46 (t, *J* = 8.4 Hz, 1H). MS (ESI) *m*/*z*: calcd for free base $C_{28}H_{38}N_4O_5$, 510.28 $[M]^+$; found, 511.5 $[M + H]^+$; $[\alpha]_D^{25}$ −41.81 (*c* 0.055, MeOH).

*(S)-5-(Azepan-1-yl)-3-(1-cyclopentyl-5-(2,6-dimethoxyphenyl)-1H-pyrazole-3-carboxamido)pentanoic Acid Hydrochloride (**11**).* Compound **11** (60 mg) was synthesized using *tert*-butyl (*S*)-3-(5-(2,6-dimethoxyphenyl)-1-cyclopentyl-1*H*-pyrazole-3-carboxamido)-5-oxopentanoate **38** (60 mg, 0.123 mmol) and azepane (11 mg, 0.148 mmol) as described in procedure **4**. 91% yield; white solid; ^{1}H NMR (MeOH-d_4, 300 MHz): δ 1.51−1.68 (m, 2H), 1.69−1.83 (m, 4H), 1.84−2.29 (m, 10H), 2.79 (d, *J* = 6.40 Hz, 2H), 3.25−3.38 (m, 4H), 3.43−3.58 (m, 3H), 3.63−3.69 (m, 2H), 3.76 (s, 6H), 4.26−4.38 (m, 1H), 4.42−4.53 (m, 1H), 6.57 (s, 1H), 6.73−6.81 (m, 2H), 7.46 (t, *J* = 8.3 Hz, 1H). MS (ESI) *m*/*z*: calcd for free base $C_{28}H_{40}N_4O_5$, 512.30 $[M]^+$; found, 513.7 $[M + H]^+$; $[\alpha]_D^{25}$ −21.43 (*c* 0.210, MeOH).

*(S)-N-(1-(Cyclobutylamino)-1-oxo-5-(pyrrolidin-1-yl)pentan-3-yl)-1-cyclopentyl-5-(2,6-dimethoxyphenyl)-1H-pyrazole-3-carboxamide Hydrochloride (**12**).* To a solution of (*S*)-3-(1-cyclopentyl-5-(2,6-dimethoxyphenyl)-1*H*-pyrazole-3-carboxamido)-5-(pyrrolidin-1-yl)pentanoic acid hydrochloride **5** (60 mg, 0.123 mol) and cyclobutylamine (12 mg, 0.161 mmol) in MeCN (5 mL) were added triethylamine (0.05 mL, 0.558 mmol) and HBTU (70 mg, 0.184 mmol). After stirring at RT for 4 h, the reaction mixture was diluted with DCM (75 mL) and washed with saturated aqueous sodium bicarbonate (75 mL). The layers were separated, and the aqueous layer was extracted with DCM (2 × 50 mL). The combined organic layers were further washed with brine, dried with Na_2SO_4, filtered, and concentrated in vacuo to give the crude product. The crude product was purified by silica gel flash column chromatography (0−40% DCM/MeOH/aq. NH_4OH (100:20:2)/DCM) to provide (*S*)-*N*-(1-(cyclobutylamino)-1-oxo-5-(pyrrolidin-1-yl)pentan-3-yl)-1-cyclopentyl-5-(2,6-dimethoxyphenyl)-1*H*-pyrazole-3-carboxamide (42 mg, 64%) as a white solid. The free base (11 mg, 0.020 mmol) was mixed with MeOH (2 mL). To it was added 2 M HCl solution in ether (0.05 mL) dropwise at room temperature and stirred for 45 min. MeOH was evaporated in vacuo and dried under high vacuum to remove all the HCl. To it was added ether, followed by trituration and filtration to obtain a white solid. The solid product was then dried under high vacuum for 16 h to give the title compound (10 mg, 85%) as a white solid. Free base ^{1}H NMR ($CDCl_3$, 300 MHz): δ 1.47−1.72 (m, 3H), 1.73−1.98 (m, 11H), 1.99−2.16 (m, 3H), 2.17−2.38 (m, 3H), 2.44−2.83 (m, 8H), 3.73 (s, 3H), 3.74 (m, 3H), 4.16−4.32 (m, 1H), 4.32−4.50 (m, 2H), 6.63 (d, *J* = 8.5 Hz, 2H), 6.66 (s, 1H), 7.01 (d, *J* = 6.4 Hz, 1H), 7.38 (t, *J* = 8.4 Hz, 1H), 8.03 (d, *J* = 7.7 Hz, 1H). MS (ESI) *m*/*z*: calcd for free base $C_{30}H_{43}N_5O_4$, 537.33 $[M]^+$; found, 538.5 $[M + H]^+$; $[\alpha]_D^{25}$ −19.75 (*c* 0.415, MeOH).

*(S)-N-(1-(Cyclobutylamino)-5-morpholino-1-oxopentan-3-yl)-1-cyclopentyl-5-(2,6-dimethoxyphenyl)-1H-pyrazole-3-carboxamide Hydrochloride (**14**).* Compound **14** (32 mg) was synthesized using (*S*)-3-(1-cyclopentyl-5-(2,6-dimethoxyphenyl)-1*H*-pyrazole-3-carboxamido)-5-morpholinopentanoic acid hydrochloride **7** (50 mg, 0.093 mmol) and cyclobutylamine (9 mg, 0.12 mmol) as described in **12**. 60% yield; white solid; Free base ^{1}H NMR ($CDCl_3$, 300 MHz): δ 1.46−1.74 (m, 7H), 1.78−1.99 (m, 7H), 2.01−2.16 (m, 2H), 2.17−3.36 (m, 2H), 2.37−2.71 (m, 8H), 3.70−3.82 (m, 2H), 3.73 (s, 3H), 3.74 (s, 3H), 4.20−4.51 (m, 3H), 6.63 (d, *J* = 8.5 Hz, 2H), 6.67 (s, 1H), 6.74−6.83 (m, 1H), 7.38 (t, *J* = 8.4 Hz, 1H), 7.88−7.97 (m, 1H). MS (ESI) *m*/*z*: calcd for free base $C_{30}H_{43}N_5O_5$, 553.33 $[M]^+$; found, 555.0 $[M + H]^+$; $[\alpha]_D^{25}$ −27.20 (*c* 0.125, MeOH).

*(S)-N-(1-(Cyclobutylamino)-5-(4-methylpiperazin-1-yl)-1-oxopentan-3-yl)-1-cyclopentyl-5-(2,6-dimethoxyphenyl)-1H-pyrazole-3-carboxamide Dihydrochloride (**15**).* Compound **15** (19 mg) was synthesized using (*S*)-3-(1-cyclopentyl-5-(2,6-dimethoxyphenyl)-1*H*-pyrazole-3-carboxamido)-5-(4-methylpiperazin-1-yl)pentanoic acid di-

https://dx.doi.org/10.1021/acs.jmedchem.0c01448
J. Med. Chem. 2021, 64, 3006−3025

hydrochloride **8** (40 mg, 0.068 mmol) and cyclobutylamine (7 mg, 0.088 mmol) as described in **12**. 49% yield; white solid; free base ^{1}H NMR ($CDCl_3$, 300 MHz): δ 1.46−1.73 (m, 9H), 1.74−1.99 (m, 6H), 2.00−2.16 (m, 2H), 2.17−2.36 (m, 4H), 2.37−2.67 (m, 9H), 3.73 (s, 3H), 3.74 (s, 3H), 4.18−4.46 (m, 3H), 6.63 (d, J = 8.5 Hz, 2H), 6.67 (s, 1H), 6.71−6.78 (m, 1H), 7.23−7.29 (m, 1H), 7.38 (t, J = 8.4 Hz, 1H), 7.53 (d, J = 8.1 Hz, 1H). MS (ESI) m/z: calcd for free base $C_{31}H_{46}N_6O_4$, 566.36 $[M]^+$; found, 567.5 $[M + H]^+$; $[\alpha]_D^{25}$ −40.80 (c 0.125, MeOH).

*N-((3S)-1-(Cyclobutylamino)-5-(2,6-dimethylpiperidin-1-yl)-1-oxopentan-3-yl)-1-cyclopentyl-5-(2,6-dimethoxyphenyl)-1H-pyrazole-3-carboxamide hydrochloride (**16**).* Compound **16** (15 mg) was synthesized using (3*S*)-3-(1-cyclopentyl-5-(2,6-dimethoxyphenyl)-1*H*-pyrazole-3-carboxamido)-5-(2,6-dimethylpiperidin-1-yl)pentanoic acid hydrochloride **9** (32 mg, 0.057 mmol) and cyclobutylamine (6 mg, 0.074 mmol) as described in **12**. 45% yield; white solid. Free base ^{1}H NMR ($CDCl_3$, 300 MHz): δ 1.15 (m, 6H), 1.22−1.42 (m, 5H), 1.44−1.75 (m, 8H), 1.75−1.99 (m, 8H), 2.18−2.36 (m, 3H), 2.55 (d, J = 6.6 Hz, 2H), 2.78−3.10 (s, 3H), 3.73 (s, 3H), 3.74 (s, 3H), 4.13−4.30 (s, 2H), 4.32−4.51 (m, 2H), 6.63 (d, J = 8.1 Hz, 2H), 6.66 (s, 1H), 7.38 (t, J = 8.4 Hz, 1H). MS (ESI) m/z: calcd for $C_{33}H_{49}N_5O_4$, 579.38 $[M]^+$; found, 580.8 $[M + H]^+$; $[\alpha]_D^{25}$ −21.53 (c 0.065, MeOH).

*(S)-N-(5-(7-Azabicyclo[2.2.1]heptan-7-yl)-1-(cyclobutylamino)-1-oxopentan-3-yl)-1-cyclopentyl-5-(2,6-dimethoxyphenyl)-1H-pyrazole-3-carboxamide Hydrochloride (**17**).* Compound **17** (13 mg) was synthesized using (*S*)-5-(7-azabicyclo[2.2.1]heptan-7-yl)-3-(1-cyclopentyl-5-(2,6-dimethoxyphenyl)-1*H*-pyrazole-3-carboxamido)-pentanoic acid hydrochloride **10** (35 mg, 0.064 mmol) and cyclobutylamine (6 mg, 0.083 mmol) as described in **12**. 36% yield; white solid; free base ^{1}H NMR ($CDCl_3$, 300 MHz): δ 1.18−1.40 (m, 8H), 1.46−1.72 (m, 7H), 1.72−1.96 (m, 4H), 1.98−2.16 (m, 2H), 2.18−2.37 (m, 2H), 2.45−2.72 (m, 4H), 3.27−3.37 (m, 2H), 3.72 (s, 3H), 3.74 (s, 3H), 4.17−4.30 (m, 2H), 4.31−4.52 (m, 2H), 6.63 (d, J = 8.5 Hz, 2H), 6.67 (s, 1H), 7.04 (d, J = 8.1 Hz, 1H), 7.37 (t, J = 8.2 Hz, 1H), 8.06 (d, J = 8.3 Hz, 1H). MS (ESI) m/z: calcd for free base $C_{32}H_{45}N_5O_4$, 563.35 $[M]^+$; found, 564.5 $[M + H]^+$; $[\alpha]_D^{25}$ −42.00 (c 0.100, MeOH).

*(S)-N-(5-(Azepan-1-yl)-1-(cyclobutylamino)-1-oxopentan-3-yl)-1-cyclopentyl-5-(2,6-dimethoxyphenyl)-1H-pyrazole-3-carboxamide Hydrochloride (**18**).* Compound **18** (30 mg) was synthesized using (*S*)-5-(azepan-1-yl)-3-(1-cyclopentyl-5-(2,6-dimethoxyphenyl)-1*H*-pyrazole-3-carboxamido)pentanoic acid hydrochloride **11** (60 mg, 0.109 mmol) and cyclobutylamine (10 mg, 0.142 mmol) as described in **12**. 48% yield; off-white solid; Free base ^{1}H NMR ($CDCl_3$, 300 MHz): δ 1.44−1.74 (m, 11H), 1.78−1.98 (m, 7H), 1.99−2.18 (m, 3H), 2.18−2.36 (m, 3H), 2.48−2.78 (m, 8H), 3.73 (s, 6H), 4.18−4.30 (m, 1H), 4.32−4.49 (m, 2H), 6.62 (d, J = 8.5 Hz, 2H), 6.67 (s, 1H), 7.03 (d, J = 8.5 Hz, 1H), 7.38 (t, J = 8.4 Hz, 1H), 8.05 (d, J = 8.3 Hz, 1H). MS (ESI) m/z: calcd for free base $C_{32}H_{47}N_5O_4$, 565.36 $[M]^+$; found, 566.5 $[M + H]^+$; $[\alpha]_D^{25}$ −32.00 (c 0.100, MeOH).

*(S)-Cyclobutyl 3-(1-cyclopentyl-5-(2,6-dimethoxyphenyl)-1H-pyrazole-3-carboxamido)-5-(piperidin-1-yl)pentanoate (**19**).* Compound **19** (21 mg) was synthesized from (*S*)-3-(1-cyclopentyl-5-(2,6-dimethoxyphenyl)-1*H*-pyrazole-3-carboxamido)-5-(piperidin-1-yl)-pentanoic acid hydrochloride **6** (35 mg, 0.065 mmol) and cyclobutanol (6 mg, 0.084 mmol) using procedure as described in 20. 58% yield; white solid; ^{1}H NMR ($CDCl_3$, 300 MHz): δ 1.37−1.49 (m, 2H), 1.50−1.68 (m, 6H), 1.73−1.98 (m, 9H), 2.00−2.18 (m, 4H), 2.27−2.52 (m, 7H), 2.54−2.78 (m, 2H), 3.73 (s, 3H), 3.74 (m, 3H), 4.20−4.30 (m, 1H), 4.45−4.57 (m, 1H), 5.01 (quin, J = 7.6 Hz, 1H), 6.63 (d, J = 8.3 Hz, 2H), 6.67 (s, 1H), 7.37 (t, J = 8.5 Hz, 1H), 7.73 (d, J = 8.9 Hz, 1H). MS (ESI) m/z: calcd for $C_{31}H_{44}N_4O_5$, 552.33 $[M]^+$; found, 553.8 $[M + H]^+$; $[\alpha]_D^{25}$ −11.02 (c 0.100, MeOH).

*(S)-1-Cyclopentyl-N-(1-((3,3-difluorocyclobutyl)amino)-1-oxo-5-(piperidin-1-yl)pentan-3-yl)-5-(2,6-dimethoxyphenyl)-1H-pyrazole-3-carboxamide (**20**).* To a solution of crude (*S*)-3-(5-(2,6-dimethoxyphenyl)-1-cyclopentyl-1*H*-pyrazole-3-carboxamido)-5-(piperidin-1-yl)pentanoic acid hydrochloride **6** (40 mg, 0.075 mmol) and 3,3-difluorocyclobutan-1-amine (14 mg, 0.097 mmol) in MeCN (4 mL) were added triethylamine (0.06 mL, 0.45 mmol) and HBTU (43 mg, 0.112 mmol). After stirring at room temperature for 4 h, the reaction mixture was diluted with water (50 mL). The layers were separated, and the aqueous layer was extracted with EtOAc (3 × 50 mL). The combined organic layers were further washed with brine (50 mL). The organic layer was separated, dried with Na_2SO_4, filtered, and concentrated in vacuo to give the crude product. The crude product was purified by silica gel flash column chromatography (0−30% DCM/MeOH/aq. NH_4OH (100:20:2)/DCM). Purified fractions were combined and concentrated to afford pure product **20** as a white solid (30 mg). 68% yield; white solid; ^{1}H NMR ($CDCl_3$, 300 MHz): δ 1.38−1.50 (m, 2H), 1.51−1.77 (m, 8H), 1.82−1.99 (m, 5H), 2.00−2.16 (m, 2H), 2.32−2.71 (m, 9H), 2.80−2.99 (m, 3H), 3.73 (s, 2H), 3.74 (s, 3H), 4.16−4.31 (m, 2H), 4.46 (m, 1H), 6.63 (d, J = 8.3 Hz, 2H), 6.67 (s, 1H), 7.38 (t, J = 8.4 Hz, 1H), 7.66 (d, J = 6.8 Hz, 1H), 8.20 (d, J = 8.3 Hz, 1H). MS (ESI) m/z: calcd for $C_{31}H_{43}F_2N_5O_4$, 587.33 $[M]^+$; found, 588.4 $[M + H]^+$; $[\alpha]_D^{25}$ −23.07 (c 0.065, MeOH).

*(S)-N-(1-(Cyclobutyl(methyl)amino)-1-oxo-5-(piperidin-1-yl)-pentan-3-yl)-1-cyclopentyl-5-(2,6-dimethoxyphenyl)-1H-pyrazole-3-carboxamide (**21**).* Compound **21** (18 mg) was synthesized from (*S*)-3-(1-cyclopentyl-5-(2,6-dimethoxyphenyl)-1*H*-pyrazole-3-carboxamido)-5-(piperidin-1-yl)pentanoic acid hydrochloride **6** (35 mg, 0.065 mmol) and *N*-methylcyclobutanamine (7 mg, 0.084 mmol) using procedure as described in **20**. 49% yield; white solid; ^{1}H NMR ($CDCl_3$, 300 MHz): δ 1.40−1.77 (m, 8H), 1.82−1.98 (m, 6H), 2.00−2.30 (m, 7H), 2.35−2.73 (m, 7H), 2.86−3.05 (m, 2H), 2.91 (s, 3H), 3.72 (s, 6H), 4.18−4.29 (m, 1H), 4.33−4.46 (m, 1H), 4.49−4.66 (m, 1H), 6.62 (d, J = 8.5 Hz, 2H), 6.66 (d, J = 3.0 Hz, 1H), 7.37 (t, J = 8.4 Hz, 1H), 8.05−8.23 (m, 1H). MS (ESI) m/z: calcd for $C_{32}H_{47}N_5O_4$, 565.36 $[M]^+$; found, 566.4 $[M + H]^+$; $[\alpha]_D^{25}$ −5.18 (c 0.135, MeOH).

*(S)-1-Cyclopentyl-5-(2,6-dimethoxyphenyl)-N-(1-((1-methylcyclobutyl)amino)-1-oxo-5-(piperidin-1-yl)pentan-3-yl)-1H-pyrazole-3-carboxamide (**22**).* Compound **22** (30 mg) was synthesized from (*S*)-3-(1-cyclopentyl-5-(2,6-dimethoxyphenyl)-1*H*-pyrazole-3-carboxamido)-5-(piperidin-1-yl)pentanoic acid hydrochloride **6** (40 mg, 0.074 mmol) and 1-methylcyclobutan-1-amine (8 mg, 0.097 mmol) using procedure as described in **20**. 71% yield; off-white solid; ^{1}H NMR ($CDCl_3$, 300 MHz): δ 1.42 (s, 3H), 1.54−1.81 (m, 5H), 1.81−2.13 (m, 12H), 2.17−2.31 (m, 3H), 2.32−2.64 (m, 10H), 3.72 (m, 3H), 3.73 (m, 3H), 4.24 (dt, J = 15.4, 7.7 Hz, 1H), 4.30−4.42 (m, 1H), 6.55 (s, 1H), 6.63 (d, J = 8.5 Hz, 2H), 6.67 (s, 1H), 7.37 (t, J = 8.4 Hz, 1H), 8.04 (d, J = 7.9 Hz, 1H). MS (ESI) m/z: calcd for $C_{32}H_{47}N_5O_4$, 565.36 $[M]^+$; found, 566.4 $[M + H]^+$; $[\alpha]_D^{25}$ −14.00 (c 0.100, MeOH).

*(S)-1-Cyclopentyl-5-(2,6-dimethoxyphenyl)-N-(1-((3-methyloxetan-3-yl)amino)-1-oxo-5-(piperidin-1-yl)pentan-3-yl)-1H-pyrazole-3-carboxamide (**23**).* Compound **23** (20 mg) was synthesized from (*S*)-3-(1-cyclopentyl-5-(2,6-dimethoxyphenyl)-1*H*-pyrazole-3-carboxamido)-5-(piperidin-1-yl)pentanoic acid hydrochloride **6** (40 mg, 0.075 mmol) and 3-methyloxetan-3-amine (9 mg, 0.097 mmol) using procedure as described in **20**. 48% yield; white solid; ^{1}H NMR ($CDCl_3$, 300 MHz): δ 1.39−1.59 (m, 5H), 1.69 (s, 3H), 1.55−1.75 (m, 5H), 1.80−2.00 (m, 5H), 2.00−2.19 (m, 2H), 2.30−2.52 (m, 5H), 2.52−2.72 (m, 3H), 3.74 (s, 6H), 4.19−4.30 (m, 1H), 4.37−4.48 (m, 3H), 4.78 (d, J = 6.4 Hz, 2H), 6.63 (d, J = 8.5 Hz, 1H), 6.66 (s, 1H), 7.38 (t, J = 8.4 Hz, 1H), 7.57−7.70 (m, 1H), 8.23 (d, J = 8.1 Hz, 1H). MS (ESI) m/z: calcd for $C_{31}H_{45}N_5O_5$, 567.34 $[M]^+$; found, 568.7 $[M + H]^+$; $[\alpha]_D^{25}$ = −18.18 (c 0.110, MeOH).

*(S)-1-Cyclopentyl-5-(2,6-dimethoxyphenyl)-N-(1-((1-methylcyclopropyl)amino)-1-oxo-5-(piperidin-1-yl)pentan-3-yl)-1H-pyrazole-3-carboxamide (**24**).* Compound **24** (18 mg) was synthesized from (*S*)-3-(1-cyclopentyl-5-(2,6-dimethoxyphenyl)-1*H*-pyrazole-3-carboxamido)-5-(piperidin-1-yl)pentanoic acid hydrochloride **6** (40 mg, 0.075 mmol) and 1-methylcyclopropan-1-amine (11 mg, 0.097 mmol) using procedure as described in **20**. 44% yield; white solid; ^{1}H NMR ($CDCl_3$, 300 MHz): δ 0.54−0.62 (m, 2H), 0.66−0.75 (m, 2H), 0.80−0.98 (m, 1H), 1.34 (s, 3H), 1.40−1.59 (m, 4H), 1.59−1.79 (m, 5H), 1.80−1.99 (m, 5H), 2.00−2.17 (m, 2H), 2.39−2.68 (m, 7H), 3.73 (s, 6H), 4.19−4.40 (m, 2H), 6.63 (d, J = 8.48 Hz, 2H), 6.65 (s, 1H), 6.89 (br s, 1H), 7.38 (t, J = 8.4 Hz, 1H), 7.98 (d, J = 7.9 Hz, 1H). MS (ESI) m/z: calcd for $C_{31}H_{45}N_5O_4$, 551.35 $[M]^+$; found, 552.9 $[M + H]^+$; $[\alpha]_D^{25}$ = −18.00 (c 0.100, MeOH).

(S)-1-Cyclopentyl-5-(2,6-dimethoxyphenyl)-N-(1-((2-methoxyethyl)(methyl)amino)-1-oxo-5-(piperidin-1-yl)pentan-3-

https://dx.doi.org/10.1021/acs.jmedchem.0c01448
J. Med. Chem. 2021, 64, 3006−3025

*yl)-1H-pyrazole-3-carboxamide (**25**).* Compound **25** (24 mg) was synthesized from (*S*)-3-(1-cyclopentyl-5-(2,6-dimethoxyphenyl)-1*H*-pyrazole-3-carboxamido)-5-(piperidin-1-yl)pentanoic acid hydrochloride **6** (35 mg, 0.065 mmol) and 2-methoxy-*N*-methylethan-1-amine (7 mg, 0.084 mmol) using procedure as described in **20**. 65% yield; colorless foam; ^{1}H NMR ($CDCl_3$, 300 MHz): δ 1.38−1.58 (m, 3H), 1.58−1.75 (m, 3H), 1.80−2.21 (m, 10H), 2.35−2.53 (m, 4H), 2.53−2.69 (m, 2H), 2.88−3.01 (m, 2H), 3.11−3.20 (m, 2H), 3.33 (d, J = 6.0 Hz, 3H), 3.46−3.55 (m, 2H), 3.49 (s, 3H), 3.73 (s, 6H), 4.19−4.29 (m, 1H), 4.37−4.52 (m, 1H), 6.62 (d, J = 8.3 Hz, 2H), 6.66 (s, 1H), 7.37 (t, J = 8.4 Hz, 1H), 8.03−8.14 (m, 1H). MS (ESI) m/z: calcd for $C_{31}H_{47}N_5O_5$, 569.36 $[M]^+$; found, 570.9 $[M + H]^+$; $[\alpha]_D^{25}$ = −15.29 (*c* 0.085, MeOH).

*(S)-1-Cyclopentyl-5-(2,6-dimethoxyphenyl)-N-(1-((2-methoxyethyl)amino)-1-oxo-5-(piperidin-1-yl)pentan-3-yl)-1H-pyrazole-3-carboxamide (**26**).* Compound **26** (19 mg) was synthesized from (*S*)-3-(1-cyclopentyl-5-(2,6-dimethoxyphenyl)-1*H*-pyrazole-3-carboxamido)-5-(piperidin-1-yl)pentanoic acid hydrochloride **6** (35 mg, 0.065 mmol) and 2-methoxyethan-1-amine (6.4 mg, 0.085 mmol) using procedure as described in **20**. 52% yield; colorless foam; ^{1}H NMR ($CDCl_3$, 300 MHz): δ 1.39−1.58 (m, 4H), 1.67 (d, J = 4.9 Hz, 5H), 1.81−1.99 (m, 6H), 2.01−2.18 (m, 2H), 2.36−2.75 (m, 7H), 3.29 (m, 3H), 3.38−3.52 (m, 4H), 3.72 (s, 3H), 3.74 (s, 3H), 4.18−4.32 (m, 1H), 4.36−4.49 (m, 1H), 6.63 (d, J = 8.5 Hz, 2H), 6.66 (s, 1H), 6.81 (br s, 1H), 7.37 (t, J = 8.4 Hz, 1H), 8.00 (d, J = 7.9 Hz, 1H). MS (ESI) m/z: calcd for $C_{30}H_{45}N_5O_5$, 555.34 $[M]^+$; found, 557.1 $[M + H]^+$; $[\alpha]_D^{25}$ = −12.29 (*c* 0.740, MeOH).

*(S)-1-Cyclopentyl-5-(2,6-dimethoxyphenyl)-N-(1-oxo-5-(piperidin-1-yl)-1-(2-oxa-6-azaspiro[3.3]heptan-6-yl)pentan-3-yl)-1H-pyrazole-3-carboxamide (**27**).* Compound **27** (25 mg) was synthesized from (*S*)-3-(1-cyclopentyl-5-(2,6-dimethoxyphenyl)-1*H*-pyrazole-3-carboxamido)-5-(piperidin-1-yl)pentanoic acid hydrochloride **6** (35 mg, 0.065 mmol) and 2-oxa-6-azaspiro[3.3]heptane (7.2 mg, 0.085 mmol) using procedure as described in **20**. 66% yield; white solid; ^{1}H NMR ($CDCl_3$, 300 MHz): δ 1.43 (m, 2H), 1.51−1.70 (m, 6H), 1.79−2.00 (m, 6H), 2.00−2.16 (m, 2H), 2.31−2.45 (m, 6H), 2.48−2.68 (m, 2H), 3.73 (s, 6H), 4.13 (s, 2H), 4.18−4.47 (m, 4H), 4.71 (s, 2H), 4.65−4.77 (m, 2H), 6.67 (s, 1H), 6.63 (d, J = 8.3 Hz, 2H), 7.37 (t, J = 8.4 Hz, 1H), 7.95 (d, J = 8.5 Hz, 1H). MS (ESI) m/z: calcd for $C_{32}H_{45}N_5O_5$, 579.34 $[M]^+$; found, 580.7 $[M + H]^+$; $[\alpha]_D^{25}$ = −7.87 (*c* 0.080, MeOH).

*(S)-1-Cyclopentyl-5-(2,6-dimethoxyphenyl)-N-(1-((oxazol-2-ylmethyl)amino)-1-oxo-5-(piperidin-1-yl)pentan-3-yl)-1H-pyrazole-3-carboxamide (**28**).* Compound **28** (27 mg) was synthesized from (*S*)-3-(1-cyclopentyl-5-(2,6-dimethoxyphenyl)-1*H*-pyrazole-3-carboxamido)-5-(piperidin-1-yl)pentanoic acid hydrochloride **6** (35 mg, 0.065 mmol) and oxazol-2-ylmethanamine (8 mg, 0.084 mmol) using procedure as described in **20**. 72% yield; white solid; ^{1}H NMR ($CDCl_3$, 300 MHz): δ 1.37−1.73 (m, 8H), 1.77−1.98 (m, 6H), 2.00−2.18 (m, 2H), 2.33−2.80 (m, 8H), 3.74 (s, 6H), 4.24 (quin, J = 7.6 Hz, 1H), 4.42−4.53 (m, 1H), 4.58 (d, J = 5.7 Hz, 2H), 6.63 (d, J = 8.48 Hz, 2H), 6.65 (s, 1H), 6.99 (s, 1H), 7.38 (t, J = 8.4 Hz, 1H), 7.45−7.54 (m, 1H), 7.71 (t, J = 5.65 Hz, 1H), 8.07−8.21 (m, 1H). MS (ESI) m/z: calcd for $C_{31}H_{42}N_6O_5$, 578.32 $[M]^+$; found, 579.9 $[M + H]^+$; $[\alpha]_D^{25}$ = −20.95 (*c* 0.105, MeOH).

*(S)-1-Cyclopentyl-5-(2,6-dimethoxyphenyl)-N-(1-oxo-5-(piperidin-1-yl)-1-(thiazol-2-ylamino)pentan-3-yl)-1H-pyrazole-3-carboxamide (**29**).* Compound **29** (19 mg) was synthesized from (*S*)-3-(1-cyclopentyl-5-(2,6-dimethoxyphenyl)-1*H*-pyrazole-3-carboxamido)-5-(piperidin-1-yl)pentanoic acid hydrochloride **6** (40 mg, 0.074 mmol) and thiazol-2-amine (9.7 mg, 0.097 mmol) using procedure as described in **20**. 44% yield; white solid; ^{1}H NMR ($CDCl_3$, 300 MHz): δ 1.40−1.59 (m, 4H), 1.68 (m, 6H), 1.80−1.97 (m, 6H), 2.00−2.19 (m, 2H), 2.35−2.66 (m, 5H), 2.77 (dd, J = 15.2, 6.1 Hz, 1H), 2.98 (dd, J = 15.3, 5.3 Hz, 1H), 3.73 (s, 6H), 4.19−4.31 (m, 1H), 4.42−4.56 (m, 1H), 6.63 (d, J = 8.5 Hz, 2H), 6.74 (s, 1H), 6.93 (d, J = 3.6 Hz, 1H), 7.38 (t, J = 8.3 Hz, 1H), 7.47 (d, J = 3.6 Hz, 1H), 8.41 (br s, 1H). MS (ESI) m/z: calcd for $C_{30}H_{40}N_6O_4S$, 580.28 $[M]^+$; found, 582.0 $[M + H]^+$; $[\alpha]_D^{25}$ = −25.00 (*c* 0.020, MeOH).

*(S)-1-Cyclopentyl-5-(2,6-dimethoxyphenyl)-N-(1-(methyl(thiazol-2-yl)amino)-1-oxo-5-(piperidin-1-yl)pentan-3-yl)-1H-pyrazole-3-carboxamide (**30**).* Compound **30** (7 mg) was synthesized from (*S*)-3-(1-cyclopentyl-5-(2,6-dimethoxyphenyl)-1*H*-pyrazole-3-carboxamido)-5-(piperidin-1-yl)pentanoic acid hydrochloride **6** (30 mg, 0.056 mmol) and *N*-methylthiazol-2-amine (8.3 mg, 0.072 mmol) using procedure as described in **20**. 22% yield; white solid; ^{1}H NMR ($CDCl_3$, 300 MHz): δ 1.38−1.49 (br s, 2H), 1.49−1.71 (m, 5H), 1.81−1.98 (m, 5H), 1.98−2.18 (m, 3H), 2.33−2.53 (m, 5H), 2.55−2.68 (m, 1H), 2.77−2.94 (m, 1H), 3.28−3.40 (m, 2H), 3.73 (s, 3H), 3.72 (s, 3H), 3.85 (s, 3H), 4.18−4.32 (m, 1H), 4.50−4.61 (m, 1H), 6.63 (d, J = 8.5 Hz, 2H), 6.68 (s, 1H), 6.99 (d, J = 3.4 Hz, 1H), 7.37 (t, J = 8.4 Hz, 1H), 7.51 (d, J = 3.6 Hz, 1H), 8.31 (d, J = 7.0 Hz, 1H). MS (ESI) m/z: calcd for $C_{31}H_{42}N_6O_4S$, 594.30 $[M]^+$; found, 595.6 $[M + H]^+$; $[\alpha]_D^{25}$ = −5.71 (*c* 0.105, MeOH).

*(S)-N-(1-((1H-Tetrazol-5-yl)amino)-1-oxo-5-(piperidin-1-yl)pentan-3-yl)-1-cyclopentyl-5-(2,6-dimethoxyphenyl)-1H-pyrazole-3-carboxamide (**31**).* Compound **31** (18 mg) was synthesized from (*S*)-3-(1-cyclopentyl-5-(2,6-dimethoxyphenyl)-1*H*-pyrazole-3-carboxamido)-5-(piperidin-1-yl)pentanoic acid hydrochloride **6** (35 mg, 0.065 mmol) and 1*H*-tetrazol-5-amine (7.2 mg, 0.085 mmol) using procedure as described in **20**. 49% yield; white solid; ^{1}H NMR ($CDCl_3$, 300 MHz): δ 1.47−1.61 (m, 3H), 1.73−2.02 (m, 9H), 2.03−2.22 (m, 3H), 2.59−2.91 (m, 4H), 2.99−3.22 (m, 3H), 3.24−3.40 (m, 2H), 3.73 (s, 3H), 3.77 (s, 3H), 4.19−4.31 (m, 2H), 4.64−4.81 (s, 1H), 6.63 (dd, J = 8.5, 3.20 Hz, 2H), 6.69 (s, 1H), 7.38 (t, J = 8.5 Hz, 1H), 7.61 (s, 1H). 13.63 (br s, 1H). (MS ESI) m/z: calcd for $C_{28}H_{39}N_9O_4$, 565.31 $[M]^+$; found, 566.5 $[M + H]^+$; $[\alpha]_D^{25}$ = −36.00 (*c* 0.125, MeOH).

*(S)-N-(1-(((1H-Tetrazol-5-yl)methyl)amino)-1-oxo-5-(piperidin-1-yl)pentan-3-yl)-1-cyclopentyl-5-(2,6-dimethoxyphenyl)-1H-pyrazole-3-carboxamide (**32**).* Compound **32** (32 mg) was synthesized from (*S*)-3-(1-cyclopentyl-5-(2,6-dimethoxyphenyl)-1*H*-pyrazole-3-carboxamido)-5-(piperidin-1-yl)pentanoic acid hydrochloride **6** (35 mg, 0.065 mmol) and (1*H*-tetrazol-5-yl)methanamine (8.4 mg, 0.085 mmol) using procedure as described in **20**. 84% yield; off-white solid; ^{1}H NMR ($CDCl_3$, 300 MHz): δ 1.47−1.58 (m, 2H), 1.58−1.73 (br s, 2H), 1.81−2.16 (m, 10H), 2.94−3.04 (m, 4H), 3.06−3.34 (m, 4H), 3.49 (s, 2H), 3.74 (m, 6H), 4.17−4.32 (m, 2H), 4.37−4.50 (m, 1H), 4.56−4.70 (m, 2H), 6.64 (d, J = 8.5 Hz, 2H), 6.62 (m, 1H), 7.37 (t, J = 8.4 Hz, 1H), 8.21−8.24 (m, 1H), 8.88−8.98 (m, 1H). MS (ESI) m/z: calcd for $C_{29}H_{41}N_9O_4$, 579.33 $[M]^+$; found, 580.7 $[M + H]^+$; $[\alpha]_D^{25}$ = −21.66 (*c* 0.060, MeOH).

*(S)-N-(1-((2-(1H-Tetrazol-5-yl)ethyl)amino)-1-oxo-5-(piperidin-1-yl)pentan-3-yl)-1-cyclopentyl-5-(2,6-dimethoxyphenyl)-1H-pyrazole-3-carboxamide (**33**).* Compound **33** (25 mg) was synthesized from (*S*)-3-(1-cyclopentyl-5-(2,6-dimethoxyphenyl)-1*H*-pyrazole-3-carboxamido)-5-(piperidin-1-yl)pentanoic acid hydrochloride **6** (35 mg, 0.065 mmol) and 2-(1*H*-tetrazol-5-yl)ethan-1-amine (10 mg, 0.085 mmol) using procedure as described in **20**. 64% yield; white solid; ^{1}H NMR ($CDCl_3$, 300 MHz): δ 1.46−1.58 (m, 2H), 1.60−1.75 (br s, 2H), 1.81−2.16 (m, 8H), 2.37−2.68 (m, 11H), 3.04−3.28 (m, 6H), 3.55−3.68 (m, 1H), 3.74 (s, 3H), 3.73 (s, 3H), 4.16−4.31 (m, 1H), 4.33−4.46 (m, 1H), 6.63 (d, J = 8.5 Hz, 2H), 6.66 (s, 1H), 7.38 (t, J = 8.4 Hz, 1H), 7.55 (br s, 1H). MS (ESI) m/z: calcd for $C_{30}H_{43}N_9O_4$, 593.34 $[M]^+$; found, 594.5 $[M + H]^+$; $[\alpha]_D^{25}$ = −42.00 (*c* 0.100, MeOH).

*(S)-1-Cyclopentyl-5-(2,6-dimethoxyphenyl)-N-(4-(piperidin-1-yl)-1-(4H-1,2,4-triazol-3-yl)butan-2-yl)-1H-pyrazole-3-carboxamide (**34**).* Step 1: Synthesis of (*S*)-*N*-(1-amino-1-oxo-5-(piperidin-1-yl)pentan-3-yl)-1-cyclopentyl-5-(2,6-dimethoxyphenyl)-1*H*-pyrazole-3-carboxamide (**48**): To a solution of (*S*)-3-(1-cyclopentyl-5-(2,6-dimethoxyphenyl)-1*H*-pyrazole-3-carboxamido)-5-(piperidin-1-yl)-pentanoic acid hydrochloride **6** (1.0 g, 1.8 mmol) in pyridine (20 mL) and dioxane (20 mL) were added ammonium carbonate (0.21 g, 2.7 mmol), followed by Boc_2O (0.47 g, 2.16 mmol). The progress of the reaction was monitored by LC−MS. Additional ammonium carbonate and Boc_2O (2 equiv each) were added after 1 h. Stirring was continued for 12 h, and additional ammonium carbonate (2 equiv) and Boc_2O (2 equiv) were added. After further stirring for 1 h, LC−MS indicated the completion of the reaction. The mixture was concentrated to dryness, quenched with saturated aqueous $NaHCO_3$ (20 mL), and extracted with EtOAc (20 mL). The EtOAc layer was separated and dried over Na_2SO_4. The solution was filtered, concentrated, and purified using silica gel flash chromatography using 0−15% MeOH in a DCM (with

https://dx.doi.org/10.1021/acs.jmedchem.0c01448
J. Med. Chem. 2021, 64, 3006−3025

1% NH_3) solvent system to give the title product **48** (0.64 g, 69% yield) as a white solid; ^{1}H NMR ($CDCl_3$, 200 MHz): δ 1.50−2.20 (m, 11H), 2.20−2.80 (m, 8H), 3.15−3.50 (m, 2H), 3.72 (s, 6H), 4.15−4.30 (m, 1H), 4.30−4.50 (m, 1H), 5.37 (br s, 1H), 6.62 (d, J = 8.4 Hz, 2H), 6.65 (s, 1H), 7.18 (br s, 1H), 7.20−7.40 (m, 2H), 7.64 (t, J = 7.0 Hz, 1H), 8.13 (d, J = 8.4 Hz, 1H), 8.61 (d, J = 4.0 Hz, 1H). MS (ESI): m/z calcd for $C_{27}H_{39}N_5O_4$, $[M]^+$ 497.30; found, 498.3 $[M + H]^+$.

Step 2: (*S*)-1-Cyclopentyl-5-(2,6-dimethoxyphenyl)-*N*-(4-(piperidin-1-yl)-1-(4*H*-1,2,4-triazol-3-yl)butan-2-yl)-1*H*-pyrazole-3-carboxamide (34): A solution of (*S*)-*N*-(1-amino-1-oxo-5-(piperidin-1-yl)-pentan-3-yl)-1-cyclopentyl-5-(2,6-dimethoxyphenyl)-1*H*-pyrazole-3-carboxamide **48** (40 mg, 0.80 mmol) in DMF−DMA (1 mL) was heated at 120 °C for 2 h. The solution was concentrated to dryness, and the residue was dissolved in glacial acetic acid (1.0 mL), followed by the addition of $NH_2NH_2{\cdot}H_2O$ (0.10 mL). The resulting solution was heated at 90 °C for 2 h, cooled to RT, quenched with saturated aqueous $NaHCO_3$ (20 mL), and extracted with EtOAc (10 mL). The EtOAc solution was dried with Na_2SO_4, filtered, and concentrated to give the crude product. The crude product was then purified by silica gel flash chromatography using 0−15% MeOH in a DCM (with 1% NH_3) solvent system to give the title product **34** (24 mg, 57% yield) as a white solid; ^{1}H NMR ($CDCl_3$, 200 MHz): δ 1.40−2.20 (m, 16H), 2.30−2.80 (m, 6H), 3.20−3.40 (m, 2H), 3.72 (s, 6H), 4.15−4.30 (m, 1H), 4.50−4.70 (m, 1H), 6.62 (d, J = 8.6 Hz, 2H), 6.68 (s, 1H), 7.35 (t, J = 7.5 Hz, 1H), 7.91 (s, 1H), 8.20 (d, J = 8.6 Hz, 1H). MS (ESI): m/z calculated for $C_{28}H_{39}N_7O_3$, $[M]^+$ 521.31; found, 522.3 $[M + H]^+$. $[\alpha]_D^{25} = -15.00$ (c 0.060, MeOH).

*(S)-N-(1-(1,3,4-Oxadiazol-2-yl)-4-(piperidin-1-yl)butan-2-yl)-1-cyclopentyl-5-(2,6-dimethoxyphenyl)-1H-pyrazole-3-carboxamide (**35**).* Step 1: Synthesis of (*S*)-methyl 3-(1-cyclopentyl-5-(2,6-dimethoxyphenyl)-1*H*-pyrazole-3-carboxamido)-5-(piperidin-1-yl)-pentanoate (49): To a solution of (*S*)-*tert*-butyl 3-(1-cyclopentyl-5-(2,6-dimethoxyphenyl)-1*H*-pyrazole-3-carboxamido)-5-(piperidin-1-yl)pentanoate **39** (1.73 g, 5.5 mmol) in DCM (10 mL) was added TFA (2 mL, 28 mmol) and stirred at RT for 2 h. The solvent was removed to provide crude (*S*)-3-(1-cyclopentyl-5-(2,6-dimethoxyphenyl)-1*H*-pyrazole-3-carboxamido)-5-(piperidin-1-yl)pentanoic acid trifluoroacetate as a yellow solid (2.1 g), which was used as is for the next reaction without further purification; MS (ESI): m/z calcd for $C_{27}H_{38}N_4O_5$ $[M + H^+]$, 498.28; found, 499.5.

To a solution of (*S*)-3-(1-cyclopentyl-5-(2,6-dimethoxyphenyl)-1*H*-pyrazole-3-carboxamido)-5-(piperidin-1-yl)pentanoic acid trifluoroacetate (120 mg, 0.24 mmol) in MeOH (2 mL) was added sulfuric acid (con., 0.20 mL) and stirred at RT for 15 h. The solution was quenched with saturated aqueous $NaHCO_3$ (20 mL), extracted with EtOAc (10 mL), dried over Na_2SO_4, and concentrated to give crude (*S*)-methyl 3-(1-cyclopentyl-5-(2,6-dimethoxyphenyl)-1*H*-pyrazole-3-carboxamido)-5-(piperidin-1-yl)pentanoate **49** (0.11 g) as colorless oil, which was used as is for the next reaction without further purification. MS (ESI): m/z calcd for $C_{28}H_{40}N_4O_5$ $[M]^+$, 512.30; found, 513.1 $[M + H]^+$.

Step 2: Synthesis of (*S*)-1-cyclopentyl-5-(2,6-dimethoxyphenyl)-*N*-(1-hydrazinyl-1-oxo-5-(piperidin-1-yl)pentan-3-yl)-1*H*-pyrazole-3-carboxamide (50): A mixture of (*S*)-methyl 3-(1-cyclopentyl-5-(2,6-dimethoxyphenyl)-1*H*-pyrazole-3-carboxamido)-5-(piperidin-1-yl)-pentanoate **49** (0.11 g), $NH_2NH_2{\cdot}H_2O$ (1.0 mL), and EtOH (3.0 mL) was heated at 80 °C for 3 h. The solution was cooled to RT, concentrated, and purified by flash silica gel chromatography using 0−15% MeOH in a DCM (with 1% NH_3) solvent system to give (*S*)-1-cyclopentyl-5-(2,6-dimethoxyphenyl)-*N*-(1-hydrazinyl-1-oxo-5-(piperidin-1-yl)pentan-3-yl)-1*H*-pyrazole-3-carboxamide **50** (60 mg, 55% yield) as colorless foam; ^{1}H NMR ($CDCl_3$, 200 MHz): δ 1.40−2.20 (m, 18H), 2.20−2.80 (m, 6H), 3.73 (s, 6H), 3.89 (br s, 2H), 4.15−4.30 (m, 1H), 4.30−4.50 (m, 1H), 6.62 (d, J = 8.4 Hz, 2H), 6.66 (s, 1H), 7.37 (t, J = 8.4 Hz, 1H), 8.06 (d, J = 7.4 Hz, 1H), 8.37 (br s, 1H). MS (ESI): m/z calcd for $C_{27}H_{40}N_6O_4$ $[M]^+$, 512.31; found, 513.1 $[M + H]^+$.

Step 3: Synthesis of (*S*)-*N*-(1-(1,3,4-oxadiazol-2-yl)-4-(piperidin-1-yl)butan-2-yl)-1-cyclopentyl-5-(2,6-dimethoxyphenyl)-1*H*-pyrazole-3-carboxamide (35): To a solution of (*S*)-1-cyclopentyl-5-(2,6-dimethoxyphenyl)-*N*-(1-hydrazinyl-1-oxo-5-(piperidin-1-yl)pentan-3-yl)-1*H*-pyrazole-3-carboxamide **50** (50 mg, 0.10 mmol) in $CH(OMe)_3$ was added PTSA.H_2O (25 mg, 0.13 mmol). The mixture was heated at 85 °C for 2 h, cooled to RT, diluted with EtOAc (10 mL), and washed with saturated aqueous $NaHCO_3$ (10 mL). The EtOAc solution was dried over Na_2SO_4, concentrated, and purified by flash silica gel chromatography using 0−15% MeOH in DCM (with 1% NH_3) to give the title product **35** (30 mg, 59%) as white foam; ^{1}H NMR ($CDCl_3$, 200 MHz): δ 1.40−2.20 (m, 18H), 2.20−2.80 (m, 4H), 3.15−3.50 (m, 2H), 3.73 (s, 6H), 4.15−4.30 (m, 1H), 4.30−4.50 (m, 1H), 6.62 (d, J = 8.0 Hz, 2H), 6.65 (s, 1H), 7.37 (t, J = 8.4 Hz, 1H), 7.90 (d, J = 8.4 Hz, 1H), 8.36 (s, 1H). MS (ESI): m/z calcd for $C_{28}H_{38}N_6O_4$ $[M]^+$, 522.30; found, 523.2 $[M + H]^+$.

Bioassays. *Lance cAMP Accumulation Assay.* Stimulation buffer containing 1× Hank's Balanced Salt Solution (HBSS), 5 mM HEPES, 0.1% BSA stabilizer, and 0.5 mM final IBMX was prepared and titrated to pH 7.4 at room temperature. Serial dilutions of the test compounds and 300 nM forskolin, both prepared at 4× the desired final concentration in stimulation buffer, were added to a 96-well white 1/2 area microplate (PerkinElmer). A cAMP standard curve prepared at 4× the desired final concentration in stimulation buffer was added to the assay plate. The final DMSO concentration in all wells was 1.5%. Stable hAPJ-CHO cells were lifted with a nonenzymatic solution (Cell-stripper, Mediatech Inc., Orlando, FL) and spun at 270 × g for 10 min. The cell pellet was resuspended in stimulation buffer, and 4000 cells were added to each well except wells containing the cAMP standard curve. After incubating for 30 min at RT, Eu-cAMP tracer and uLIGHT-*anti*-cAMP working solutions were added as per the manufacturer's instructions. After incubation at RT for 1 h, the TR-FRET signal (ex 337 nm, em 620 and 650 nm) was read on a CLARIOstar multimode plate reader (BMG Biotech, Cary, NC). For the screen, the same procedure was followed except that instead of adding serial dilutions of the test compounds, a single concentration (1 μM, prepared at 4× final) of each test compound was added to the assay plates. Data were analyzed using Prism software (GraphPad, La Jolla, CA). Nonlinear regression analysis was performed to fit data and obtain maximum response (E_{max}), EC_{50}, correlation coefficient (r^2), and other parameters. All experiments were performed in duplicate 2−3 times to ensure reproducibility, and data are reported as mean ± s.e.m., unless noted otherwise.

Calcium Mobilization Assay. CHO cells stably expressing either the $G\alpha_{q16}$ protein (CHO-RD-HGA16; Molecular Devices) plus the human apelin receptor (CHO hAPJ), mouse apelin receptor (CHO mAPJ), or human angiotensin II receptor, type I (CHO hAGTR1; DiscoverX) were removed from flasks using Cell-stripper and quenched with DMEM/F12, 10% FBS, and 1× Penicillin/Streptomycin, centrifuged, and resuspended in the serum-containing media. Cells were counted with a hemocytometer, and 30,000 cells of CHO hAPJ and 20,000 cells of CHO hAGTR1 were transferred to each well of a black Costar 96-well optical bottom plate (Corning Corporation, Corning, NY). Each plate was incubated at 37 °C for 24 h. The culture media was removed from the plates, and cells were washed with DPBS and were subsequently loaded with a fluorescent calcium probe (Calcium 5 dye; Molecular Devices, Sunnyvale, CA) in an HBSS-based buffer containing 20 mM HEPES, 1% BSA, and 10 μM probenecid (Sigma) in a total volume of 225 μL with the final DMSO concentration at 1%. Cells were incubated at 37 °C for 1 h and then stimulated with test compounds or pyr-apelin-13 (Anaspec, Freemont, CA) at various concentrations using an FLIPR Tetra plate reader. Agonist-mediated change in fluorescence (ex 488 nm, em 525 nm) was monitored in each well at 1 s intervals for 90 s. Data were collected using Softmax version 4.8 (MDS Analytical Technologies) and analyzed using Prism software. Nonlinear regression analysis was performed to fit data and obtain maximum response (E_{max}), EC_{50}, correlation coefficient (r^2), and other parameters. All experiments were performed in duplicate 2−3 times to ensure reproducibility, and data are reported as mean ± s.e.m., unless noted otherwise.

PathHunter β-Arrestin-2 Recruitment Assay. The stable CHO-K1 human AGTRL1 β-arrestin-2 cell line (DiscoverX) was maintained in TC-treated flasks with growth media containing DMEM/F12 (Corning Cellgro, Manassas, VA), 10% FBS, and 1× Penicillin-streptomycin L-

https://dx.doi.org/10.1021/acs.jmedchem.0c01448
J. Med. Chem. 2021, 64, 3006−3025

glutamine (Gibco, Carlsbad, CA). The selection reagents used were geneticin (800 μg/mL) and hygromycin (300 μg/mL). The cells were removed from the flasks using a Cell-stripper. Cells were resuspended in complete media and spun at 300*g* for 5 min. The supernatant was discarded, and cells were resuspended in Assay Complete Cell plating 2 Reagent (DiscoverX). Cells were counted using a hemocytometer and seeded in a white clear bottom TC-treated 96-well plate (DiscoverX) at 10,000 cells per well. The plates were incubated at 37 °C and 5% CO_2 for 24 h. Compound dilutions were prepared at 10× final in DPBS (1×) buffer with 10% DMSO and 1% BSA. Compound dilutions were added to the 80−90% confluent assay plate, and the plates were incubated at 37 °C and 5% CO_2 for 90 min, followed by the addition of PathHunter Detection Reagent (DiscoverX), prepared as per the manufacturer's instructions. The assays were run at 1% DMSO and 0.1% BSA final. The culture plates were incubated another 60 min at room temperature. The luminescent signal was detected on an Enspire multimode plate reader (PerkinElmer CT, USA). Data were collected using EnSpire Software 4.1 and analyzed using GraphPad Prism. Nonlinear regression analysis was performed to fit data and obtain maximum response (E_{max}), EC_{50}, correlation coefficient (r^2), and other parameters. All experiments were performed in duplicate at least two times to ensure reproducibility, and data are reported as mean ± s.e.m., unless noted otherwise.

[^{35}S]GPTγS Binding Assay. The [^{35}S]GPTγS assays were conducted using the methods previously reported.[49] Briefly, the binding of the GTP analogue [^{35}S]GPTγS to the membrane was determined in a volume of 500 μL. The assay mixture contained 50 mM HEPES (pH 7.4), 100 mM NaCl, 5 mM $MgCl_2$, 1 mM EDTA·$2H_2O$, 1 mM dithiothreitol, 0.1% BSA, 10 μM GDP, test compounds, and approximately 132,000 cpm of [35S]-GTPγS (0.1 nM). Human apelin 2 μg (per assay tube) APJ receptor-expressing CHO-K1 cell membranes were added to each tube. For the apelin receptor assays, seven-point concentration response curves of the agonist Pyr-aplein-13 (1 μM, 100 nM, 10 nM, 1 nM, 0.1 nM, 0.01 nM, and 0.001 nM) were prepared, and the dilutions were coincubated with a seven-point concentration curve of the test compound (31.6 μM, 10 μM, 3.16 μM, 316 nM, 100 nM, 31.6 nM, 3.16 nM, and 0.316 nM final). Following a 60 min shaking incubation at 22 °C, the assay was terminated by filtration under vacuum on a Brandel (Gaithersburg, MD, USA) 96-well harvester using presoaked PerkinElmer GF/B glass-fiber filters. The filters were rinsed three times with 1 mL washes of ice-cold wash buffer (20 mM HEPES pH 7.4, 100 mM NaCl, and 10 mM $MgCl_2$). Filter plates were dried for 1 h at 55 °C. Microscint 20 (50 μL) was added to each well, and filter-bound radioactivity was counted on a Packard Top Count NXT microplate scintillation and luminescence counter. Total binding (TB) was determined in the absence of compounds, and nonspecific binding (NSB) was determined in the presence of 10 μM final unlabeled GTPγS. Percent specific bound (SB) was calculated using the equation % SB = (SB/MB) × 100, where maximal binding (MB) is calculated by subtracting NSB from TB. Percent SB was plotted against the log of compound concentration. Data were fit to a three-parameter logistic curve to generate EC_{50} values (GraphPad Prism, GraphPad Software, Inc., San Diego, CA). K_e values were calculated using the equation $K_e = [L]/((EC_{50+}/EC_{50-}) - 1)$ where $[L]$ is the concentration of the test compound, EC_{50+} is the EC_{50} of the control agonist with the test compound, and EC_{50-} is the EC_{50} of the control agonist alone. K_e values were considered valid when the EC_{50+}/EC_{50-} ratio was at least 4. All experiments were performed in duplicate 2−3 times to ensure reproducibility, and data are reported as mean ± s.e.m., unless noted otherwise.

MDCK-MDR1 Assay. MDCK-mdr1 cells obtained from The Netherlands Cancer Institute were grown on Transwell type filters (Corning) for 4 d to confluence in DMEM/F12 media containing 10% fetal bovine serum and antibiotics. Compounds were added to the apical side at a concentration of 10 μM in a transport buffer composed of 1× Hank's balanced salt solution, 25 mM D-glucose, and buffered with HEPES to pH 7.4. Samples were incubated for 1 h at 37 °C and carefully collected from both the apical and basal sides of the filters. Compounds selected for MDCK-mdr1 cell assays were infused on an Applied Biosystems API-4000 mass spectrometer to optimize for analysis using multiple reaction monitoring. The chromatography was conducted with an Agilent 1100 binary pump with a flow rate of 0.5 mL/min. The mobile phase solvents were 0.1% formic acid in water (A) and 0.1% formic acid in methanol (B). The solvent conditions were 10% B for 1 min, followed by a gradient to 95% B over 5 min. Data reported are average values of two to three measurements.

Plasma Protein Binding Assay. Compounds were diluted in plasma at a concentration of 10 μM. A total of 100 μL of the compound in plasma was placed into the sample chamber of a Thermo Fisher Scientific RED Device (Waltham, MA). A total of 350 μL of dialysis buffer (PBS containing 100 mM sodium phosphate and 150 mM sodium chloride) was added to the buffer chamber. The plate was covered with sealing tape and incubated at 37 °C for 4 h at 100 rpm in a shaking incubator. Fifty microliters of postdialysis samples from the buffer and the plasma chambers were pipetted into separate microfuge tubes. Fifty microliters of plasma was added to the buffer sample, and 50 μL of buffer was added to the plasma sample. Three hundred microliters of ice-cold 90/10 acetonitrile/water with 0.1% formic acid was added to precipitate protein and release compound. Samples were centrifuged at 13,000*g* for 10 min and transferred to LC−MS/MS vials for analysis. Samples were analyzed with an SCIEX 6500 + UHPLC/MS system (Framingham, MA). Experiments were performed with three independent samples.

Radioligand Displacement Assay for hERG Interaction. Competition binding with [^{3}H] astemizole was used to measure hERG interaction, as has been previously described.[43] Preparations of membranes overexpressing hERG were purchased from PerkinElmer. The binding assays were performed for 60 min using 4 μg of hERG-expressing membranes, ∼3 nM [^{3}H]astemizole, and various concentrations of the test agent in a pH 7.4 buffer (10 mM HEPES, 130 mM NaCl, 5 mM KCl, 0.8 mM $MgCl_2$, 1 mM NaEDTA, 10 mM glucose, and 0.1% BSA). Binding was terminated by rapid filtration onto GF/B fiber filter mats (presoaked in 0.3% polyethyleneimine), followed by rapid washing (6 × 2 mL) with an ice-cold pH 7.4 buffer (25 mM Tris−HCl, 130 mM NaCl, 5 mM KCl, 0.8 mM $MgCl_2$, 0.05 mM $CaCl_2$, and 0.1% BSA) using a Brandel harvester. Filters were dried and counted after the addition of a scintillant. Data were analyzed using nonlinear regression (GraphPad Prism) and K_i values. All experiments were performed at least twice in duplicate, and the data reported are the mean values.

Human Microsomal Stability Studies. Human microsomal stability assays were performed as described previously.[50] Briefly, test compounds were incubated at a 1 μM final concentration with 0.5 mg/mL pooled human liver microsomes from 200 unidentified donors (Xenotech, LLC, Lenexa, KS) in a 100 mM phosphate buffer (pH 7.4) containing 3 mM $MgCl_2$, 1 mM nicotinamide adenine dinucleotide phosphate (NADPH), 5 mM uridine diphosphate glucuronic acid, and 50 μg/mL alamethicin. Triplicate samples were incubated for up to 120 min. Samples were removed at regular intervals. Reactions were terminated by the addition of 3 volumes of methanol and processed for LC−MS by centrifugation. Standard curves were prepared in the blank matrix for each compound for quantitative assessment. The intrinsic clearance rate was calculated for each compound using the formula: Clint (μL/min/mg) = $0.693/(t_{1/2} \times$ microsomal protein concentration). Data reported are average values from 3 measurements.

Kinetic Solubility Determination. The kinetic solubility of the test compound was measured in commercial phosphate buffer saline (PBS, pH 7.4), which consisted of potassium phosphate monobasic 1 mM, sodium phosphate dibasic 3 mM, and sodium chloride 155 mM. A 10 μL of the test compound stock solution (20 mM DMSO) was combined with 490 μL of PBS buffer to reach a targeted concentration of 400 μM. The solution was agitated on a VX-2500 multitube vortexer (VWR) for 2 h at room temperature. Following agitation, the sample was filtered on a glass-fiber filter (1 μm) and the eluate was diluted 400-fold with a mixture of acetonitrile/water (1:1). On each experimental occasion, nicardipine and imipramine were assessed as reference compounds for low and high solubility, respectively. All samples were assessed in triplicate and analyzed by LC−MS/MS using electrospray ionization against standards prepared in the same matrix.

PK Analysis. Male CD-1 mice were ordered from Charles River Laboratories and allowed to acclimate to the facility for 72 h. Mice were aged around 10 weeks and were dosed with compound **13** formulated in

https://dx.doi.org/10.1021/acs.jmedchem.0c01448
J. Med. Chem. 2021, 64, 3006−3025

modified citrate buffer (pH: 6) via IP (15 mg/kg). Animals were sacrificed at multiple time points (0.5, 1, 2, 4, 8, and 24 h), and samples were removed. PK analyses were performed as described in our previous publications using Phoenix WinNonlin (Certara).[51]

DIO Study. All studies were performed in accordance with guidelines established by the Office of Laboratory Animal Welfare (OLAW) and protocols were approved by the institutional animal care and use committee (IACUC). Preconditioned male C57BL6J mice were purchased from the Jackson Laboratories (Bar Harbor, Maine) at 18 weeks of age. Power analysis was performed to refine study design and optimize animal usage using SAS software (Cary, NC). We assumed 9 animals per group. This gave the study >80% statistical power assuming 40% change effect, 25% deviation, 5% alpha error level (95% confidence) in a two-tailed design. These animals were maintained either on ad libitum normal diet with 10% fat (D12450B) or on 60% fat (D12492) chow from Research Diets (New Brunswick, NJ). Animals were acclimated to the facility for two weeks and then randomly assigned to various test groups (9−10 animals per group). Animals were housed individually in polycarbonate cages. Animals were dosed with a citrate-buffered vehicle (10 mM citrate buffer with 40 mg/mL D-mannitol adjusted to pH 3) or **13** dissolved the vehicle BID by i.p. dosing for 28 consecutive days. Dosing volume was maintained at 5 mL/kg. Body weights were taken at regular intervals and food consumption tracked. Animals were food-deprived for 12 h prior to the oral glucose tolerance test (GTT). For GTT, animals were orally dosed with a 2 g/kg bolus dose of glucose in water. Using a fine scissors, tails were snipped (<1 mm) once, the same snipped area was used for subsequent blood collection. A very small sample size of approximately 2−5 μL of blood was used. Measurements were performed using a glucometer and standard blood glucose measurement strips at 15, 30, 60, 90, 120 min, post challenge. At termination of study, plasma and vital organs were collected and preserved appropriately. Serum samples from each animal were analyzed for alanine aminotransferase (ALT), free FA, and LDH levels by an independent laboratory (MPI Research/Charles River Laboratories, Mattawan, MI) using good laboratory practice. Tissue sections (10 μm) from frozen livers were prepared and analyzed following hematoxylin−eosin staining and Oil Red O staining using standard procedures. Data were graphed using Prism software (GraphPad, La Jolla, CA), and statistical analyses were performed using the same program. Triglyceride levels were measured using a commercially available colorimetric kit from Cayman Chemicals (Cat # 10010303, Ann Arbor, MI).

■ ASSOCIATED CONTENT

Supporting Information

The Supporting Information is available free of charge at https://pubs.acs.org/doi/10.1021/acs.jmedchem.0c01448.

^{1}H NMR, mass, and HPLC trace of compound **13**; safety screen data of compound **13**; PK analysis of compound **13**; and HPLC trace of target compounds (PDF)

List of molecular formula strings (CSV)

■ AUTHOR INFORMATION

Corresponding Authors

Scott P. Runyon − *Center for Drug Discovery, RTI International, Durham, North Carolina 27709, United States*; Phone: 919-316-3842; Email: srunyon@rti.org; Fax: 919-541-8868

Rangan Maitra − *Center for Drug Discovery, RTI International, Durham, North Carolina 27709, United States*; orcid.org/0000-0001-6663-6800; Phone: 919-541-6795; Email: rmaitra@rti.org; Fax: 919-541-8868

Authors

Sanju Narayanan − *Center for Drug Discovery, RTI International, Durham, North Carolina 27709, United States*

Shaobin Wang − *Center for Drug Discovery, RTI International, Durham, North Carolina 27709, United States*

Vineetha Vasukuttan − *Center for Drug Discovery, RTI International, Durham, North Carolina 27709, United States*

Ravi Kumar Vyas Devambatla − *Sterling Pharma Solutions Limited, Cary, North Carolina 27513, United States*

Donghua Dai − *Sterling Pharma Solutions Limited, Cary, North Carolina 27513, United States*

Chunyang Jin − *Center for Drug Discovery, RTI International, Durham, North Carolina 27709, United States*; orcid.org/0000-0001-6733-3094

Rodney Snyder − *Center for Drug Discovery, RTI International, Durham, North Carolina 27709, United States*

Lucas Laudermilk − *Center for Drug Discovery, RTI International, Durham, North Carolina 27709, United States*

Complete contact information is available at: https://pubs.acs.org/10.1021/acs.jmedchem.0c01448

Funding

This work was supported by NIH grant: 1R01DK103625.

Notes

The authors declare no competing financial interest.

■ ACKNOWLEDGMENTS

Authors wish to thank Dr. Elaine Gay, Dr. Ann Decker, Nigel Edgerton, and Taylor Rosa for help with various assays.

■ ABBREVIATIONS

AT1, angiotensin 1; ALT, alanine aminotransferase; Boc_2O, di-*tert*-butyl dicarbonate; CHO-K1, chinese hamster ovary cells; DCE, 1,2-dichloroethane; DCM/CH_2Cl_2, dichloromethane; DMF, *N*,*N*-dimethylformamide; DMF−DMA, *N*,*N*-dimethylformamide dimethyl acetal; DIO, drug-induced obesity; EtOAc, ethyl acetate; EtOH, ethanol; Et_3N, triethylamine; HBTU, *N*,*N*,*N*′,*N*′-tetramethyl-*O*-(1*H*-benzotriazol-1-yl)uronium hexafluorophosphate; HCl, hydrochloric acid; HFD, high-fat diet; LiOH·H_2O, lithium hydroxide monohydrate; MeCN, acetonitrile; MeOH, methanol; MDCK-mdr1, Madin−Darby canine kidney cells transfected with the human MDR1 gene; NaBH(OAc)$_3$, sodium triacetoxyborohydride; $(NH_4)_2CO_3$, ammonium carbonate; $Na_2S_2O_3$, sodium thiosulfate; NaOH, sodium hydroxide; NH_4OH, ammonium hydroxide; $NaHCO_3$, sodium bicarbonate; PTSA·H_2O, *p*-toluenesulfonic acid monohydrate; PPB, plasma protein binding; SAR, structure−activity relationship; TFA, trifluoroacetic acid; THF, tetrahydrofuran; TLC, thin-layer chromatography

■ REFERENCES

(1) Aguilar-Salinas, C. A.; Viveros-Ruiz, T., Recent Advances in Managing/Understanding the Metabolic Syndrome. *F1000Research* **2019**, *8*. DOI: 10.12688/f1000research.17122.1

(2) Wysocka, M. B.; Pietraszek-Gremplewicz, K.; Nowak, D. The Role of Apelin in Cardiovascular Diseases, Obesity and Cancer. *Front. Physiol.* **2018**, *9*, 557.

(3) Pitkin, S. L.; Maguire, J. J.; Bonner, T. I.; Davenport, A. P. International Union of Basic and Clinical Pharmacology. Lxxiv. Apelin Receptor Nomenclature, Distribution, Pharmacology, and Function. *Pharmacol. Rev.* **2010**, *62*, 331−342.

(4) Narayanan, S.; Harris, D. L.; Maitra, R.; Runyon, S. P. Regulation of the Apelinergic System and Its Potential in Cardiovascular Disease: Peptides and Small Molecules as Tools for Discovery. *J. Med. Chem.* **2015**, *58*, 7913−7927.

(5) Iturrioz, X.; Alvear-Perez, R.; De Mota, N.; Franchet, C.; Guillier, F.; Leroux, V.; Dabire, H.; Le Jouan, M.; Chabane, H.; Gerbier, R.; Bonnet, D.; Berdeaux, A.; Maigret, B.; Galzi, J. L.; Hibert, M.; Llorens-Cortes, C. Identification and Pharmacological Properties of E339-3d6, the First Nonpeptidic Apelin Receptor Agonist. *FASEB J.* **2010**, *24*, 1506−1517.
(6) Khan, P.; Maloney, P. R.; Hedrick, M.; Gosalia, P.; Milewski, M.; Li, L.; Roth, G. P.; Sergienko, E.; Suyama, E.; Sugarman, E.; Nguyen, K.; Mehta, A.; Vasile, S.; Su, Y.; Shi, S.; Stonich, D.; Nguyen, H.; Zeng, F. Y.; Novo, A. M.; Vicchiarelli, M.; Diwan, J.; Chung, T. D. Y.; Pinkerton, A. B.; Smith, L. H. Functional Agonists of the Apelin (APJ) Receptor. *Probe Reports from the NIH Molecular Libraries Program*; U.S. National Library of Medicine: Bethesda (MD), 2010.
(7) Hachtel, S. W., Wolfart, P.; Weston, J.; Mueller, M.; Defossa, E.; Mertsch, K.; Weng, J. H.; Binnie, R. A.; Abdul-Latif, F.; Bock, W. J.; Walser, A. Benzimidazolecarboxylic Acid Amino Acid Amides as Apelin Receptor Modulators. WO 2014044738 A1, 2014.
(8) Pinkerton, A. B. S.; Smith, L. H. Agonist of the Apelin Receptor and Methods of Use Thereof. WO 2015184011 A2, 2015.
(9) Meng, W.; Chao, H. J.; Finlay, H.; Lawrence, R. M.; Myers, M. C., Apelin Receptor Agonists and Methods of Use. WO 2017096130 A1; Bristo-Myers Squibb Company, 2017.
(10) Chen, X.; Chen, Y.; Cheng, A. C.; Connors, R. V.; Debenedetti, M. V.; Dransfield, P. J.; Fu, Z.; Harvey, J. S.; Heath, J. A.; Hedley, S. J.; Houze, J.; Judd, T. C.; Khakoo, A. Y.; Kopecky, D. J.; Lai, S.-J.; Ma, Z.; Nishimura, N.; Olson, S. H.; Pattaropong, V.; Swaminath, G.; Wang, X.; Yeh, W.-C. Heterocyclic Triazole Compounds as Agonists of the APJ Receptor. WO 2017192485 A1; Amgen Inc, 2017.
(11) Narayanan, S.; Vasukuttan, V.; Rajagopal, S.; Maitra, R.; Runyon, S. P. Identification of Potent Pyrazole Based Apelin Receptor (APJ) Agonists. *Bioorg. Med. Chem.* **2020**, *28*, 115237.
(12) De Mota, N.; Lenkei, Z.; Llorens-Cortès, C. Cloning, Pharmacological Characterization and Brain Distribution of the Rat Apelin Receptor. *Neuroendocrinology* **2000**, *72*, 400−407.
(13) Medhurst, A. D.; Jennings, C. A.; Robbins, M. J.; Davis, R. P.; Ellis, C.; Winborn, K. Y.; Lawrie, K. W. M.; Hervieu, G.; Riley, G.; Bolaky, J. E.; Herrity, N. C.; Murdock, P.; Darker, J. G. Pharmacological and Immunohistochemical Characterization of the APJ Receptor and its Endogenous Ligand Apelin. *J. Neurochem.* **2003**, *84*, 1162−1172.
(14) Bodineau, L.; Taveau, C.; Lê Quan Sang, H.-H.; Osterstock, G.; Queguiner, I.; Moos, F.; Frugière, A.; Llorens-Cortes, C. Data Supporting a New Physiological Role for Brain Apelin in the Regulation of Hypothalamic Oxytocin Neurons in Lactating Rats. *Endocrinology* **2011**, *152*, 3492−3503.
(15) Galanth, C.; Hus-Citharel, A.; Li, B.; Llorens-Cortes, C. Apelin in the Control of Body Fluid Homeostasis and Cardiovascular Functions. *Curr. Pharm. Des.* **2012**, *18*, 789−798.
(16) Llorens-Cortes, C.; Kordon, C. Jacques Benoit Lecture: The Neuroendocrine View of the Angiotensin and Apelin Systems. *J. Neuroendocrinol.* **2008**, *20*, 279−289.
(17) Castan-Laurell, I.; Dray, C.; Attané, C.; Duparc, T.; Knauf, C.; Valet, P. Apelin, Diabetes, and Obesity. *Endocrine* **2011**, *40*, 1−9.
(18) Rayalam, S.; Della-Fera, M. A.; Krieg, P. A.; Cox, C. M.; Robins, A.; Baile, C. A. A Putative Role for Apelin in the Etiology of Obesity. *Biochem. Biophys. Res. Commun.* **2008**, *368*, 815−819.
(19) Boucher, J.; Masri, B.; Daviaud, D.; Gesta, S.; Guigné, C.; Mazzucotelli, A.; Castan-Laurell, I.; Tack, I.; Knibiehler, B.; Carpéné, C.; Audigier, Y.; Saulnier-Blache, J.-S.; Valet, P. Apelin, a Newly Identified Adipokine Up-Regulated by Insulin and Obesity. *Endocrinology* **2005**, *146*, 1764−1771.
(20) Guo, L.; Li, Q.; Wang, W.; Yu, P.; Pan, H.; Li, P.; Sun, Y.; Zhang, J. Apelin Inhibits Insulin Secretion in Pancreatic Beta-Cells by Activation of Pi3-Kinase-Phosphodiesterase 3b. *Endocr. Res.* **2009**, *34*, 142−154.
(21) Sörhede Winzell, M.; Magnusson, C.; Ahrén, B. The APJ Receptor Is Expressed in Pancreatic Islets and Its Ligand, Apelin, Inhibits Insulin Secretion in Mice. *Regul. Pept.* **2005**, *131*, 12−17.
(22) Dray, C.; Debard, C.; Jager, J.; Disse, E.; Daviaud, D.; Martin, P.; Attané, C.; Wanecq, E.; Guigné, C.; Bost, F.; Tanti, J.-F.; Laville, M.; Vidal, H.; Valet, P.; Castan-Laurell, I. Apelin and Apj Regulation in Adipose Tissue and Skeletal Muscle of Type 2 Diabetic Mice and Humans. *Am. J. Physiol.: Endocrinol. Metab.* **2010**, *298*, E1161−E1169.
(23) Dray, C.; Knauf, C.; Daviaud, D.; Waget, A.; Boucher, J.; Buléon, M.; Cani, P. D.; Attané, C.; Guigné, C.; Carpéné, C.; Burcelin, R.; Castan-Laurell, I.; Valet, P. Apelin Stimulates Glucose Utilization in Normal and Obese Insulin-Resistant Mice. *Cell Metab.* **2008**, *8*, 437−445.
(24) Higuchi, K.; Masaki, T.; Gotoh, K.; Chiba, S.; Katsuragi, I.; Tanaka, K.; Kakuma, T.; Yoshimatsu, H. Apelin, an APJ Receptor Ligand, Regulates Body Adiposity and Favors the Messenger Ribonucleic Acid Expression of Uncoupling Proteins in Mice. *Endocrinology* **2007**, *148*, 2690−2697.
(25) Attane, C.; Foussal, C.; Le Gonidec, S.; Benani, A.; Daviaud, D.; Wanecq, E.; Guzman-Ruiz, R.; Dray, C.; Bezaire, V.; Rancoule, C.; Kuba, K.; Ruiz-Gayo, M.; Levade, T.; Penninger, J.; Burcelin, R.; Penicaud, L.; Valet, P.; Castan-Laurell, I. Apelin Treatment Increases Complete Fatty Acid Oxidation, Mitochondrial Oxidative Capacity, and Biogenesis in Muscle of Insulin-Resistant Mice. *Diabetes* **2012**, *61*, 310−320.
(26) Yue, P.; Jin, H.; Xu, S.; Aillaud, M.; Deng, A. C.; Azuma, J.; Kundu, R. K.; Reaven, G. M.; Quertermous, T.; Tsao, P. S. Apelin Decreases Lipolysis Via G(Q), G(I), and Ampk-Dependent Mechanisms. *Endocrinology* **2011**, *152*, 59−68.
(27) Yue, P.; Jin, H.; Aillaud, M.; Deng, A. C.; Azuma, J.; Asagami, T.; Kundu, R. K.; Reaven, G. M.; Quertermous, T.; Tsao, P. S. Apelin is Necessary for the Maintenance of Insulin Sensitivity. *Am. J. Physiol.: Endocrinol. Metab.* **2010**, *298*, E59−E67.
(28) Than, A.; Cheng, Y.; Foh, L.-C.; Leow, M. K.-S.; Lim, S. C.; Chuah, Y. J.; Kang, Y.; Chen, P. Apelin Inhibits Adipogenesis and Lipolysis through Distinct Molecular Pathways. *Mol. Cell. Endocrinol.* **2012**, *362*, 227−241.
(29) Kidoya, H.; Naito, H.; Takakura, N. Apelin Induces Enlarged and Nonleaky Blood Vessels for Functional Recovery from Ischemia. *Blood* **2010**, *115*, 3166−3174.
(30) Kidoya, H.; Ueno, M.; Yamada, Y.; Mochizuki, N.; Nakata, M.; Yano, T.; Fujii, R.; Takakura, N. Spatial and Temporal Role of the Apelin/APJ System in the Caliber Size Regulation of Blood Vessels During Angiogenesis. *EMBO J.* **2008**, *27*, 522−534.
(31) Sawane, M.; Kajiya, K.; Kidoya, H.; Takagi, M.; Muramatsu, F.; Takakura, N. Apelin Inhibits Diet-Induced Obesity by Enhancing Lymphatic and Blood Vessel Integrity. *Diabetes* **2013**, *62*, 1970−1980.
(32) Yamamoto, T.; Habata, Y.; Matsumoto, Y.; Yasuhara, Y.; Hashimoto, T.; Hamajyo, H.; Anayama, H.; Fujii, R.; Fuse, H.; Shintani, Y.; Mori, M. Apelin-Transgenic Mice Exhibit a Resistance against Diet-Induced Obesity by Increasing Vascular Mass and Mitochondrial Biogenesis in Skeletal Muscle. *Biochim. Biophys. Acta* **2011**, *1810*, 853−862.
(33) Charo, D. N.; Ho, M.; Fajardo, G.; Kawana, M.; Kundu, R. K.; Sheikh, A. Y.; Finsterbach, T. P.; Leeper, N. J.; Ernst, K. V.; Chen, M. M.; Ho, Y. D.; Chun, H. J.; Bernstein, D.; Ashley, E. A.; Quertermous, T. Endogenous Regulation of Cardiovascular Function by Apelin-APJ. *Am. J. Physiol.: Heart Circ. Physiol.* **2009**, *297*, H1904−H1913.
(34) Kasai, A.; Shintani, N.; Kato, H.; Matsuda, S.; Gomi, F.; Haba, R.; Hashimoto, H.; Kakuda, M.; Tano, Y.; Baba, A. Retardation of Retinal Vascular Development in Apelin-Deficient Mice. *Arterioscler., Thromb., Vasc. Biol.* **2008**, *28*, 1717−1722.
(35) Japp, A. G.; Cruden, N. L.; Amer, D. A. B.; Li, V. K. Y.; Goudie, E. B.; Johnston, N. R.; Sharma, S.; Neilson, I.; Webb, D. J.; Megson, I. L.; Flapan, A. D.; Newby, D. E. Vascular Effects of Apelin in Vivo in Man. *J. Am. Coll. Cardiol.* **2008**, *52*, 908−913.
(36) Barnes, G. D.; Alam, S.; Carter, G.; Pedersen, C. M.; Lee, K. M.; Hubbard, T. J.; Veitch, S.; Jeong, H.; White, A.; Cruden, N. L.; Huson, L.; Japp, A. G.; Newby, D. E. Sustained Cardiovascular Actions of APJ Agonism during Renin-Angiotensin System Activation and in Patients with Heart Failure. *Circ.: Heart Failure* **2013**, *6*, 482−491.
(37) Japp, A. G.; Cruden, N. L.; Barnes, G.; van Gemeren, N.; Mathews, J.; Adamson, J.; Johnston, N. R.; Denvir, M. A.; Megson, I. L.; Flapan, A. D.; Newby, D. E. Acute Cardiovascular Effects of Apelin in

https://dx.doi.org/10.1021/acs.jmedchem.0c01448
J. Med. Chem. 2021, 64, 3006−3025

Humans: Potential Role in Patients with Chronic Heart Failure. *Circulation* **2010**, *121*, 1818−1827.
(38) Szokodi, I.; Tavi, P.; Földes, G.; Voutilainen-Myllylä, S.; Ilves, M.; Tokola, H.; Pikkarainen, S.; Piuhola, J.; Rysä, J.; Tóth, M.; Ruskoaho, H. Apelin, the Novel Endogenous Ligand of the Orphan Receptor APJ, Regulates Cardiac Contractility. *Circ. Res.* **2002**, *91*, 434−440.
(39) Maguire, J. J.; Kleinz, M. J.; Pitkin, S. L.; Davenport, A. P. [Pyr1]Apelin-13 Identified as the Predominant Apelin Isoform in the Human Heart: Vasoactive Mechanisms and Inotropic Action in Disease. *Hypertension* **2009**, *54*, 598−604.
(40) Messari, S. E.; Iturrioz, X.; Fassot, C.; De Mota, N.; Roesch, D.; Llorens-Cortes, C. Functional Dissociation of Apelin Receptor Signaling and Endocytosis: Implications for the Effects of Apelin on Arterial Blood Pressure. *J. Neurochem.* **2004**, *90*, 1290−1301.
(41) Ceraudo, E.; Galanth, C.; Carpentier, E.; Banegas-Font, I.; Schonegge, A.-M.; Alvear-Perez, R.; Iturrioz, X.; Bouvier, M.; Llorens-Cortes, C. Biased Signaling Favoring Gi over Beta-Arrestin Promoted by an Apelin Fragment Lacking the C-Terminal Phenylalanine. *J. Biol. Chem.* **2014**, *289*, 24599−24610.
(42) Besserer-Offroy, É.; Bérubé, P.; Côté, J.; Murza, A.; Longpré, J.-M.; Dumaine, R.; Lesur, O.; Auger-Messier, M.; Leduc, R.; Marsault, É.; Sarret, P. The Hypotensive Effect of Activated Apelin Receptor is Correlated with Beta-Arrestin Recruitment. *Pharmacol. Res.* **2018**, *131*, 7−16.
(43) Chiu, P. J. S.; Marcoe, K. F.; Bounds, S. E.; Lin, C.-H.; Feng, J.-J.; Lin, A.; Cheng, F.-C.; Crumb, W. J.; Mitchell, R. Validation of a [3H]Astemizole Binding Assay in HEK293 Cells Expressing Herg K+ Channels. *J. Pharmacol. Sci.* **2004**, *95*, 311−319.
(44) Carroll, F. I.; Gichinga, M. G.; Kormos, C. M.; Maitra, R.; Runyon, S. P.; Thomas, J. B.; Mascarella, S. W.; Decker, A. M.; Navarro, H. A. Design, Synthesis, and Pharmacological Evaluation of Jdtic Analogs to Examine the Significance of the 3- and 4-Methyl Substituents. *Bioorg. Med. Chem.* **2015**, *23*, 6379−6388.
(45) Amato, G.; Manke, A.; Wiethe, R.; Vasukuttan, V.; Snyder, R.; Yueh, Y. L.; Decker, A.; Runyon, S.; Maitra, R. Functionalized 6-(Piperidin-1-Yl)-8,9-Diphenyl Purines as Peripherally Restricted Inverse Agonists of the CB1 Receptor. *J. Med. Chem.* **2019**, *62*, 6330−6345.
(46) Davies, S. G.; Mulvaney, A. W.; Russell, A. J.; Smith, A. D. Parallel Synthesis of Homochiral B-Amino Acids. *Tetrahedron: Asymmetry* **2007**, *18*, 1554−1566.
(47) O'Carroll, A.-M.; Lolait, S. J.; Harris, L. E.; Pope, G. R. The Apelin Receptor APJ: Journey from an Orphan to a Multifaceted Regulator of Homeostasis. *J. Endocrinol.* **2013**, *219*, R13−R35.
(48) Chaves-Almagro, C.; Castan-Laurell, I.; Dray, C.; Knauf, C.; Valet, P.; Masri, B. Apelin Receptors: From Signaling to Antidiabetic Strategy. *Eur. J. Pharmacol.* **2015**, *763*, 149−159.
(49) Kormos, C. M.; Ondachi, P. W.; Runyon, S. P.; Thomas, J. B.; Mascarella, S. W.; Decker, A. M.; Navarro, H. A.; Carroll, F. I. Simple Tetrahydroisoquinolines Are Potent and Selective Kappa Opioid Receptor Antagonists. *ACS Med. Chem. Lett.* **2017**, *8*, 742−745.
(50) Fulp, A.; Bortoff, K.; Seltzman, H.; Zhang, Y.; Mathews, J.; Snyder, R.; Fennell, T.; Maitra, R. Design and Synthesis of Cannabinoid Receptor 1 Antagonists for Peripheral Selectivity. *J. Med. Chem.* **2012**, *55*, 2820−2834.
(51) Fulp, A.; Bortoff, K.; Zhang, Y.; Seltzman, H.; Mathews, J.; Snyder, R.; Fennell, T.; Maitra, R. Diphenyl Purine Derivatives as Peripherally Selective Cannabinoid Receptor 1 Antagonists. *J. Med. Chem.* **2012**, *55*, 10022−10032.

https://dx.doi.org/10.1021/acs.jmedchem.0c01448
J. Med. Chem. 2021, 64, 3006−3025